

69-19,069

THAILER, Henry Jules, 1935-
ON BENDING OF CURVED TUBES.

The City University of New York, Ph.D., 1969
Engineering Mechanics

University Microfilms, Inc., Ann Arbor, Michigan

ON BENDING OF CURVED TUBES

by

HENRY J. THAILER¹²⁵

A dissertation submitted to the Graduate Faculty in Engineering in partial fulfillment of the requirements for the degree of Doctor of Philosophy, The City University of New York.

1969

This manuscript has been read and accepted for the Graduate Faculty in Engineering in satisfaction of the dissertation requirement for the degree of Doctor of Philosophy.

May 2, 1969
Date

2 May 1969
date

David H. Cheng
Chairman of Examining Committee

Leon Newman
Executive Officer

Prof. Jacques E. Benveniste

Prof. Gerard G. Lowen

Prof. Ming L. Pei

Prof. David H. Cheng, Chairman
Supervisory Committee

The City University of New York

ACKNOWLEDGMENTS

I am deeply indebted to my mentor, Professor David H. Cheng, for his patience, physical insight, and the many hours of assistance spent on the research leading to this dissertation.

The assistance and guidance of Professor Jacques E. Benveniste is also most gratefully appreciated.

The financial support of the City University of New York is gratefully acknowledged.

TABLE OF CONTENTS

| Chapter | | Page |
|---------|---|------|
| | ABSTRACT | 1 |
| 1 | INTRODUCTION | 3 |
| 2 | FORMULATION OF PROBLEM | |
| | 2.1 Geometry of Tube | 6 |
| | 2.2 Strain-Displacement Relations | 7 |
| | 2.3 Equilibrium Equations | 11 |
| | 2.4 Constitutive Relations | 13 |
| | 2.5 Differential Equations | 14 |
| | 2.6 Strain Energy | 18 |
| 3 | GENERAL SOLUTION FOR AXISYMMETRIC CASE | |
| | 3.1 Series Expansion | 20 |
| | 3.2 Application of Theorem of Minimum Complementary Energy | 21 |
| | 3.3 Stress Intensification and Rigidity Factors | 23 |
| | 3.4 Evaluation of Integrals | 25 |
| | A. Binomial Expansion | 25 |
| | B. Exact Integral | 27 |
| | 3.5 Discussion of Results | 29 |
| 4 | ASYMPTOTIC SOLUTION FOR AXISYMMETRIC CASE | |
| | 4.1 Theory and Solution | 33 |
| | 4.2 Discussion of Results | 36 |
| 5 | ASYMMETRIC CASE | |
| | 5.1 Displacements | 41 |
| | 5.2 Application of Theorem of Minimum Potential Energy | 42 |
| | 5.3 Discussion of Results | 46 |
| | FIGURES | 49 |
| | BIBLIOGRAPHY | 63 |
| | VITA | 65 |

LIST OF FIGURES

| <u>Figure Number</u> | <u>Title</u> | <u>Page Number</u> |
|--------------------------|---|------------------------|
| 1. | Geometry of Tube | 49 |
| 2. | Rigidity Factor vs. μ - Binomial Expansion | 50 |
| 2A. | Rigidity Factor vs. μ - Exact Integral | 51 |
| 3. | Meridional Stress Intensification Factor ($\lambda = 0.339$, $\mu = 36.9$) | 52 |
| 4. | Longitudinal Stress Intensification Factor ($\lambda = 0.339$, $\mu = 36.9$) | 53 |
| 5. | Meridional Stress Intensification Factor ($\lambda = 0.512$, $\mu = 46.2$) | 54 |
| 6. | Longitudinal Stress Intensification Factor ($\lambda = 0.512$, $\mu = 46.2$) | 55 |
| 7. | λ - Effect on Meridional Stress Intensification Factor ($\mu = 100$) | 56 |
| 8. | λ - Effect on Meridional Stress Intensification Factor ($\mu = 16.5$) | 57 |
| 9. | $ S_{\phi} _{\max}$ vs. μ - General Solution and Existing Asymptotic Solutions | 58 |
| 10. | $ S_{\phi} _{\max}$ vs. μ - Modified Asymptotic Solution | 59 |
| 11. | Flexibility Factor vs. μ of a U-Bend with End Flanges | 60 |
| 12. | $ S_{\phi} _{\max}$ vs. μ of a U-Bend with End Flanges | 61 |
| 13. | $ S_{\theta} _{\max}$ vs. μ of a U-Bend with End Flanges | 62 |

NOMENCLATURE

| | | |
|---------------|---|--|
| a | - | Radius of curvature of centerline of tube |
| b | - | Radius of cross section of tube |
| D | - | $Eh^3/12(1-\nu^2)$ |
| E | - | Modulus of elasticity |
| H | - | Horizontal stress resultant |
| h | - | Thickness of tube |
| I | - | πb^3h - Moment of inertia of tube |
| m | - | In-plane moment |
| M_e | - | Longitudinal stress couple |
| M_ϕ | - | Meridional stress couple |
| N_e | - | Longitudinal normal stress resultant |
| N_ϕ | - | Meridional normal stress resultant |
| q | - | Extension of centerline of tube |
| Q_ϕ | - | Shear stress resultant |
| r | - | Radial coordinate of point on middle surface |
| S_ϕ, S_e | - | Stress intensification factor in meridional and longitudinal direction, respectively |
| U | - | Total strain energy |
| u | - | Horizontal component of displacement |
| V | - | Vertical stress resultant |

- V_c - Total complementary energy
 V_p - Total potential energy
 W - Potential energy of end moment
 w - Vertical component of displacement
 z - Vertical coordinate of point on middle surface
 α - Angular rotation of a longitudinal tangent
 Δ - Angular rotation of a plane section
 β - Angular rotation of a meridional tangent
 γ - $\frac{\sqrt{12(1-\nu^2)}}{E h^2} r H$
 ϵ_{θ_0} - Strain on middle surface in longitudinal direction
 ϵ_{ϕ_0} - Strain on middle surface in meridional direction
 κ_{θ} - Curvature change in longitudinal direction
 κ_{ϕ} - Curvature change in meridional direction
 λ - b/a , radius ratio
 μ - $\sqrt{12(1-\nu^2)} \frac{b^2}{a h}$, pipe parameter
 ν - Poisson's ratio
 η - Rigidity factor
 Φ - Flexibility factor
 θ_0 - Central angle of bend
 η - q/b

ABSTRACT

The stress distribution and flexibility of thin-walled curved circular tubes, with and without flanges, subjected to in plane end couples are investigated. The dissertation divides into two major parts:

I Axisymmetric tubes (no flanges)

a) General solution

b) Asymptotic solution for large pipe parameter, μ

II Asymmetric tubes, having the shape of U, with heavy flanges at ends.

(I) A general solution for a curved circular tube viewed as an axisymmetric thin shell of revolution is obtained. The two dependent variables are expanded in trigonometric series such that they automatically satisfy one of the two coupled ordinary differential equations, namely, the equilibrium equation regardless of the value of radius ratio, λ . It is shown that the compatibility equation would also be satisfied identically if λ is very small ($\lambda \approx 0$). The general solution is thus reduced to an existing solution valid for vanishingly small values of λ which correspond to nearly straight tubes. In order not to impose any restriction on λ , the total complementary energy is minimized in the manner of Rayleigh-Ritz to insure that the compatibility condition is satisfied. Numerical results correlate well with

experimental data. The general solution is not only more accurate, but also more rapidly convergent than other existing analytical methods.

Existing asymptotic solutions for axisymmetric tubes are re-examined and modified to reflect the effect of the radius ratio. The differential equations are integrated numerically using the Runge-Kutta method. The modified asymptotic formulas correlate very well with existing experimental results.

(II) A solution for a U-bend tube terminated by rigid end flanges is presented for the first time. Displacements and rotation are expanded in trigonometric series, thus insuring satisfaction of compatibility conditions. Equilibrium is guaranteed by minimizing the total potential energy in the manner of Rayleigh-Ritz. Numerical results are compared with experimental results.

CHAPTER 1

INTRODUCTION

A curved tube of circular cross section is more flexible in bending than a straight tube because the cross section tends to ovalize. Due to ovalization, not only is the maximum longitudinal stress higher than that predicted by the elementary theory, but it is accompanied by a meridional stress of even higher magnitude.

The analytical study of axisymmetric curved tubes has claimed efforts of many investigators. However, except for the studies by Tueda⁽¹⁾, Symond and Pardue⁽²⁾, Turner and Ford⁽³⁾, and Jones⁽⁴⁾, most are valid only for the restricted case in which the radius of the tube is small in relation to the radius of curvature of its centerline.

Based on the classical theory of thin-shells, Tueda obtained two coupled ordinary differential equations with variable coefficients, which were integrated by means of a power series of trigonometric functions. Numerical results were obtained for flexibility and stress intensification factors (ratio of stress in a curved tube to that in a straight tube) for tubes having radius ratios, λ , as large as one-fifth. It was claimed that adequate results should be obtainable for values of λ up to but less than one-half. But poor convergence was found by this writer for λ about one-third and μ about 30.

Symond and Pardue ⁽²⁾, and recently Jones ⁽⁴⁾, made an assumption imposing the inextensibility of the middle surface in the meridional direction and obtained solutions for tubes having any radius ratio by minimizing the total potential energy. Although this assumption was able to simplify the mathematics involved, it nevertheless introduced a stress distribution that underestimated the maximum stress ⁽⁵⁾⁽⁶⁾. Jones indicated that for some values of pipe parameter, μ , even a ten-term expansion was inadequate to insure proper convergence of stresses in the meridional direction. Turner and Ford ⁽³⁾ used a mechanics-of-materials approach, and by expanding four pertinent parameters in series form, obtained a solution by solving $4n+5$ simultaneous equations, where $(n+1)$ represents the number of terms in each series expansion. This method frequently requires the solution of large systems of simultaneous algebraic equations, forty-nine (49) or more are not uncommon to obtain reasonably convergent results for moderate λ and μ .

Curved tubes of relatively large λ have also been extensively studied experimentally by Gross and Ford ⁽⁵⁾, Pardue and Vigness ⁽⁶⁾, and Vissat and Del Buono ⁽⁷⁾.

In most cases, the maximum stress magnitude, if not the location, has been found to be in good agreement with the existing analytical results. But the correlation becomes increasingly more difficult as λ increases to about one-half and μ becomes large. It is not surprising

because the existing solutions, in addition to drawbacks already mentioned, become less convergent when λ and μ get large.

There has been no work published for curved tubes terminated by heavy flanges which are common occurrences in engineering applications although experimental results have long existed ⁽⁶⁾. This dissertation is sub-divided into two major parts. In part one, a general solution is given for a curved tube without end flanges subjected to in plane end couples. The problem is formulated based on the theory of axisymmetric thin shells of revolution. The solution includes that proposed by Clark and Reissner ⁽⁸⁾ as a particular case in which λ is set to zero. For large pipe parameters, the asymptotic solution given by Clark and Reissner ⁽⁸⁾ is modified to reflect the influence of λ . Both general and asymptotic solutions are compared with existing experimental results. In part two, a solution is given for a curved tube (U-bend) terminated by heavy flanges. The displacements are described by a double trigonometric expansion in both the meridional and longitudinal coordinates and the angular rotation by a single expansion. The total potential energy is minimized to insure equilibrium conditions. The results are compared with the published test results.

CHAPTER 2

FORMULATION OF PROBLEM

2.1 Geometry of Tube

Figure 1 shows a curved tube of circular cross section and uniform wall thickness, h . Consider this tube as being generated by rotating about an axis, a circular ring whose radius to the middle surface is " b ". The horizontal distance from the axis of rotation to the center of the annulus is denoted by " a ".

The principal curvilinear coordinates measured along the middle surface of the shell are: ϕ - coordinate in the meridional direction and Θ - coordinate in the longitudinal direction. The third principal coordinate, ξ , is directed normal to the middle surface. The horizontal distance from the axis of rotation to a point on the middle surface of the tube is denoted by " r ". Thus

$$r = a + b \sin \phi \quad (2-1)$$

The vertical distance from the center of the tube to a point on the middle surface is denoted by " z ".

$$z = -b \cos \phi \quad (2-2)$$

The principal radii of curvature in the meridional and longitudinal directions are, respectively:

$$\begin{aligned} R_{\phi} &= -b \\ R_{\Theta} &= \frac{-r}{\sin \phi} \end{aligned} \quad (2-3)$$

2.2 Strain-Displacement Relations

Let the displacement of a point on the middle surface of the tube in the ϕ , θ , ξ directions be denoted by w_ϕ , w_θ , w_ξ , respectively.

The succeeding derivation for thin-walled tubes will be based on the Kirchoff hypotheses, namely:

- a) Straight fibers which are perpendicular to the middle surface before deformation, remain so after deformation and do not change their length.
- b) The normal stresses acting on planes parallel to the middle surface are negligible in comparison with other stresses.

Further, the derivation and application will be restricted to problems in which the displacements are small in comparison to the thickness of the tube.

As a consequence of the Kirchoff assumptions and restricting attention to a linear theory, the displacements of points on parallel surfaces \bar{w}_ϕ , \bar{w}_θ , \bar{w}_ξ , may be written as:

$$\bar{w}_\phi = w_\phi + \beta \xi$$

$$\bar{w}_\theta = w_\theta + \alpha \xi \quad (2-4)$$

$$\bar{w}_\xi = w_\xi$$

where β and α represent the projections of the deformed unit normal to the middle surface, \bar{e}_ξ , on the directions e_ϕ and e_θ ,

respectively. The unit vectors e_ϕ, e_θ, e_z form a right-hand system. Since small displacements are assumed, these projections are equal to the angles by which, during deformation, the normal to the middle surface rotates about the axes e_ϕ and e_θ , respectively.

These rotations as well as middle surface strains may be written in terms of displacements (11) :

$$\begin{aligned} \beta &= -\frac{\partial w_z}{b \partial \phi} + \frac{w_\phi}{R_\phi} \\ \alpha &= -\frac{\partial w_z}{r \partial \theta} + \frac{w_\theta}{R_\theta} \\ \epsilon_{\phi_0} &= \frac{\partial w_\phi}{b \partial \phi} + \frac{w_z}{R_\phi} \\ \epsilon_{\theta_0} &= \frac{\partial w_\theta}{r \partial \theta} + \frac{w_\phi}{br} \frac{\partial r}{\partial \phi} + \frac{w_z}{R_\theta} \end{aligned} \quad (2-5)$$

where $\epsilon_{\phi_0}, \epsilon_{\theta_0}$ represent extensional strains at points on the middle surface in the meridional and longitudinal directions, respectively.

Imposing the basic assumptions previously stated to the parallel surfaces of the tube, one obtains:

$$\begin{aligned} \epsilon_{\phi\phi} &= \frac{1}{1 + \frac{s}{R_\phi}} \left[\epsilon_{\phi_0} + s \kappa_\phi \right] \\ \epsilon_{\theta\theta} &= \frac{1}{1 + \frac{s}{R_\theta}} \left[\epsilon_{\theta_0} + s \kappa_\theta \right] \end{aligned} \quad (2-6)$$

where

$$\kappa_{\phi} = \frac{\partial \beta}{b \partial \phi} \quad (2-7)$$

$$\kappa_{\theta} = \frac{\partial \alpha}{r \partial \theta} + \frac{1}{br} \frac{\partial r}{\partial \phi} \beta$$

The terms κ_{ϕ} and κ_{θ} may be interpreted geometrically as changes in curvature of the middle surface of the tube as it deforms (positive values indicate decreased curvature).

Since our attention is restricted to thin-walled tubes, i. e.

$t \gg \frac{s}{R}$, the strain expressions may be simplified to:

$$\epsilon_{\phi\phi} = \epsilon_{\phi_0} + s \kappa_{\phi} \quad (2-8)$$

$$\epsilon_{\theta\theta} = \epsilon_{\theta_0} + s \kappa_{\theta}$$

Let the end moments be applied in the plane of symmetry.

In the axisymmetric case, the cross sectional ovalization and displacement are independent of θ . Assuming plane sections remain plane, one writes:

$$w_{\theta} = R r \theta \quad (2-9)$$

where

$$R = \frac{\partial \Delta}{\partial \theta} = \text{constant} \quad (2-10)$$

and Δ is the rotation of a plane cross section. κ_{θ} in (2-7) may be written:

$$\kappa_{\theta} = \frac{\cos \phi}{r} \beta - \frac{k \sin \phi}{r} \quad (2-11)$$

with

$$\alpha = -\Delta \sin \phi$$

It should be noted that the second term in (2-11) does not appear in Clark and Reissner's (8) derivation. This term would disappear for complete toroidal shells; however, for incomplete toroids it should be considered.

It will be more convenient to analyze the axisymmetric problem in terms of the horizontal and vertical displacements, u and w , respectively:

$$u = w_{\phi} \cos \phi - w_z \sin \phi \quad (2-12)$$

$$w = -w_{\phi} \sin \phi - w_z \cos \phi$$

Thus, the middle surface strains and rotation become:

$$\begin{aligned} \epsilon_{\phi_0} &= \frac{1}{b \cos \phi} \left[\frac{\partial u}{\partial \phi} - b \beta \sin \phi \right] \\ \epsilon_{\theta_0} &= \frac{u}{r} + k \end{aligned} \quad (2-13)$$

where:

$$\beta = \frac{1}{b} \left[\frac{\partial u}{\partial \phi} \sin \phi + \frac{\partial w}{\partial \phi} \cos \phi \right]$$

2.3 Equilibrium Equations

Let $\sigma_{\phi\phi}$, $\sigma_{\theta\theta}$, $\sigma_{\phi\theta}$ represent the normal and shear stresses acting on an element of the tube. Consider a statically equivalent force system denoted by stress resultants and stress couples:

$$\begin{aligned}
 N_{\phi} &= \int \sigma_{\phi\phi} \left[1 + \frac{s}{R_{\theta}} \right] dS \\
 N_{\theta} &= \int \sigma_{\theta\theta} \left[1 + \frac{s}{R_{\phi}} \right] dS \\
 M_{\phi} &= \int \sigma_{\phi\phi} \left[1 + \frac{s}{R_{\theta}} \right] s dS \\
 M_{\theta} &= \int \sigma_{\theta\theta} \left[1 + \frac{s}{R_{\phi}} \right] s dS \\
 Q_{\phi} &= \int \sigma_{\phi\theta} \left[1 + \frac{s}{R_{\theta}} \right] dS
 \end{aligned} \tag{2-14}$$

where the limits of integration are from $-h/2$ to $+h/2$.

Figure 1 shows an element separated from a tube by four cuts perpendicular to the middle surface. The normal and shear stress resultants as well as stress couples, in the meridional and longitudinal directions, are shown acting on this element. It should be noted that due to axisymmetry, $\frac{\partial N_{\theta}}{\partial \theta} = \frac{\partial M_{\theta}}{\partial \theta} = Q_{\theta} = 0$. The stress resultants may be replaced by an equivalent resultant force system, V and H , in the vertical and horizontal directions respectively.

These two equivalent force systems are related by:

$$V = -N_{\phi} \sin \phi - Q_{\phi} \cos \phi \quad (2-15)$$

$$H = N_{\phi} \cos \phi - Q_{\phi} \sin \phi$$

If no pressure or other surface loading exists, then, from

Figure 1, it is clear that the force equilibrium in the radial and axial directions require that:

$$\frac{d(rV)}{d\phi} = 0 \quad (2-16)$$

$$\frac{d(rH)}{d\phi} - b N_{\theta} = 0 \quad (2-17)$$

The moment equilibrium equations reduce to resolving the moments about the e_{θ} coordinate, since, the moment about the normal coordinate is automatically satisfied while axisymmetry insures moment equilibrium about the e_{ϕ} coordinate axis. Thus:

$$\frac{d(rM_{\phi})}{d\phi} - \frac{dr}{d\phi} M_{\theta} - Q_{\phi} br = 0 \quad (2-18)$$

It is clear from (2-16) that since V vanishes at $\phi = \frac{\pi}{2}$, it vanishes everywhere. The stress resultants (2-15), thus become:

$$N_{\phi} = H \cos \phi \quad (2-19)$$

$$Q_{\phi} = -H \sin \phi$$

The resultant internal resisting moment at any cross section must be independent of Θ , a constant, and equal to the externally applied end moment, m :

$$m = \int \phi \left[N_{\Theta} r - M_{\Theta} \sin \phi \right] b d\phi \quad (2-20)$$

2.4 Constitutive Relations

The equations and solutions presented in this dissertation will be confined to homogeneous, isotropic, linearly elastic materials. The solutions will further be restricted to thin-walled tubes. Under this restriction, it is reasonable to neglect the normal stress through the thickness of the tube in comparison with the remaining stresses.

Thus, Hooke's law becomes

$$\begin{aligned} \sigma_{\phi\phi} &= \frac{E}{(1-\nu^2)} \left[\epsilon_{\phi\phi} + \nu \epsilon_{\theta\theta} \right] \\ \sigma_{\theta\theta} &= \frac{E}{(1-\nu^2)} \left[\epsilon_{\theta\theta} + \nu \epsilon_{\phi\phi} \right] \\ \sigma_{\phi\theta} &= \frac{E}{2(1+\nu)} \epsilon_{\phi\theta} \end{aligned} \quad (2-21)$$

where:

| | |
|---|--|
| $\sigma_{\phi\phi}, \sigma_{\theta\theta}, \sigma_{\phi\theta}$ | represents stresses on parallel surfaces |
| E | Modulus of Elasticity |
| ν | Poisson's Ratio |

It will be more convenient to write the constitutive relations not only in terms of stress resultants but also in terms of middle surface strains and rotations. Integrating through the thickness of the tube, one obtains:

$$\begin{aligned}
 N_{\phi} &= C \left[\epsilon_{\phi_0} + \nu \epsilon_{\theta_0} \right] \\
 N_{\theta} &= C \left[\epsilon_{\theta_0} + \nu \epsilon_{\phi_0} \right] \\
 M_{\phi} &= D \left[\kappa_{\phi} + \nu \kappa_{\theta} \right] \\
 M_{\theta} &= D \left[\kappa_{\theta} + \nu \kappa_{\phi} \right]
 \end{aligned}
 \tag{2-22}$$

where:

$$\begin{aligned}
 C &\equiv \frac{Eh}{(1-\nu^2)} \\
 D &\equiv \frac{Eh^3}{12(1-\nu^2)}
 \end{aligned}
 \tag{2-23}$$

2.5 Differential Equations

In this section, the differential equations which govern the behavior of the tube will be derived, first, in its general form; second, in simplified form; and third, for the particular case of vanishingly small radius ratio.

2.5.1 General

The general form of the governing differential equations for axisymmetric tubes is derived in this section. Substituting (2-19), (2-22), into (2-18) and using (2-7) & (2-11), the equation of equilibrium can be written as:

$$\frac{d^2\beta}{d\phi^2} + \frac{\lambda \cos\phi}{1+\lambda \sin\phi} \frac{d\beta}{d\phi} - \left[\frac{(\lambda \cos\phi)^2}{(1+\lambda \sin\phi)^2} + \frac{\nu \lambda \sin\phi}{1+\lambda \sin\phi} \right] \beta + \mu \frac{\sin\phi}{1+\lambda \sin\phi} \gamma = -\frac{k \lambda \cos\phi}{(1+\lambda \sin\phi)^2} \left[\lambda \sin\phi - \nu(1+\lambda \sin\phi) \right] \quad (2-24)$$

where:

$$\lambda = b/a$$

$$\gamma = \frac{\sqrt{12(1-\nu^2)}}{E h^2} r H \quad (2-25)$$

$$\mu = \sqrt{12(1-\nu^2)} \frac{b^2}{a h}$$

Eliminating u from (2-13) the following compatibility equation is obtained:

$$\frac{d(r\epsilon_{\theta\theta})}{d\phi} - \epsilon_{\phi\phi} \frac{dr}{d\phi} - \beta \frac{dz}{d\phi} = k \frac{dr}{d\phi} \quad (2-26)$$

Substituting (2-22) into (2-26) and using (2-17), (2-19) & (2-25)

the compatibility equation becomes:

$$\frac{d^2\gamma}{d\phi^2} + \frac{\lambda \cos\phi}{1+\lambda \sin\phi} \frac{d\gamma}{d\phi} - \left[\frac{(\lambda \cos\phi)^2}{(1+\lambda \sin\phi)^2} - \frac{\nu \lambda \sin\phi}{1+\lambda \sin\phi} \right] \gamma - \mu \frac{\sin\phi}{1+\lambda \sin\phi} \beta = \mu k \frac{\cos\phi}{1+\lambda \sin\phi} \quad (2-27)$$

$$- \mu \frac{\sin\phi}{1+\lambda \sin\phi} \beta = \mu k \frac{\cos\phi}{1+\lambda \sin\phi}$$

The coupled differential equations which govern the problem, (1) (2-24) and (2-27) were first obtained by Tueda . These equations were integrated by means of a power series of trigonometric functions and, extensive numerical tabulation of results given for values of λ as large as 1/5. Tueda claimed that adequate results should be obtainable for values of radius ratio less than 1/2, however, this writer found poor convergence for λ about one-third and μ about 30. Divergent results were found for $\lambda = 1/2$ regardless of the value of μ . (8)

Clark and Reissner obtained a similar pair of governing differential equations with the exception that the right hand side of (2-24) was zero. However, for an incomplete torus, this term would not, in general, vanish.

2.5.2 Simplified ($\lambda \neq 0$)

In order to keep λ as a parameter, it is both desirable and feasible to disregard, based on certain physical arguments, certain secondary terms so as to simplify the problem. To this end, one may observe from (2-7) & (2-11) that for thin tubes κ_{ϕ} is always predominant as compared to κ_{θ} ; hence, the third term in (2-24) is vanishingly small compared with the first two terms. Thus, making this simplification leads to the following equilibrium equation:

$$\frac{d^2\beta}{d\phi^2} + \frac{\lambda \cos \phi}{1 + \lambda \sin \phi} \frac{d\beta}{d\phi} + \mu \frac{\sin \phi}{1 + \lambda \sin \phi} \gamma = 0 \quad (2-28)$$

Similarly, one may observe that in (2-22) N_{θ} is always predominant compared with N_{ϕ} , and the third term in (2-27) is negligible with respect to the first two terms. The compatibility equation is thus simplified to:

$$\frac{d^2 \gamma}{d\phi^2} + \frac{\lambda \cos \phi}{1 + \lambda \sin \phi} \frac{d\gamma}{d\phi} - \mu \frac{\sin \phi}{1 + \lambda \sin \phi} \beta = \frac{\mu k \cos \phi}{1 + \lambda \sin \phi} \quad (2-29)$$

2.5.3 Simplified ($\lambda \doteq 0$)

The coupled ordinary differential equations (2-28) and (2-29) were first given by Clark and Reissner ⁽⁸⁾ based on a different argument. They further simplified the problem, by assuming $\lambda = 0$, and presented a solution to the following coupled ordinary differential equations:

$$\begin{aligned} \frac{d^2 \beta}{d\phi^2} + \mu \sin \phi \gamma &= 0 \\ \frac{d^2 \gamma}{d\phi^2} - \mu \sin \phi \beta &= \mu k \cos \phi \end{aligned} \quad (2-30)$$

Clearly a solution to this set of equations is valid for slightly curved tubes of vanishingly small radius ratio only.

2.6 Strain Energy

The general formula for strain energy is:

$$U = \frac{1}{2} \int \sigma_{ij} \epsilon_{ij} br \left(1 + \frac{s}{R_\phi}\right) \left(1 + \frac{s}{R_\theta}\right) d\phi d\theta ds \quad (2-31)$$

where the integration extends over the entire volume of the body.

The Kirchoff hypotheses are equivalent to neglecting the stress σ_{rs} in comparison with the remaining stresses and the strains $\epsilon_{\phi s}$, $\epsilon_{\theta s}$ in comparison with the remaining strains.

Thus it follows from these hypotheses:

$$U = \frac{1}{2} \int \left[\sigma_{\phi\phi} \epsilon_{\phi\phi} + \sigma_{\theta\theta} \epsilon_{\theta\theta} + \sigma_{\phi\theta} \epsilon_{\phi\theta} \right] \cdot \left[1 + \frac{s}{R_\phi} \right] \left[1 + \frac{s}{R_\theta} \right] br d\phi d\theta ds \quad (2-32)$$

The integrand may be written explicitly in terms of strain, and in particular the strains related to the middle surface of the tube. Integrating through the thickness of the tube and substituting (2-8) and (2-21) into (2-32) and neglecting the effect of shear:

$$U = \frac{C}{2} \int \left[\epsilon_{\phi_0}^2 + \epsilon_{\theta_0}^2 + 2\nu \epsilon_{\phi_0} \epsilon_{\theta_0} \right] br d\phi d\theta + \frac{D}{2} \int \left[\kappa_\phi^2 + \kappa_\theta^2 + 2\nu \kappa_\phi \kappa_\theta \right] br d\phi d\theta \quad (2-33)$$

where the limits of integration extend over the entire middle surface of the tube.

The complementary strain energy for a tube may be obtained by integrating through the thickness of the tube. Neglecting the contribution of shear, one gets:

$$\begin{aligned} U = & \frac{1}{2Eh} \int [N_{\phi}^2 + N_{\theta}^2 - 2\nu N_{\phi}N_{\theta}] br d\phi d\theta \\ & + \frac{6}{Eh^3} \int [M_{\phi}^2 + M_{\theta}^2 - 2\nu M_{\phi}M_{\theta}] br d\phi d\theta \end{aligned} \quad (2-34)$$

GENERAL SOLUTION FOR AXISYMMETRIC CASE

(8)
Clark and Reissner presented a solution to the pair of differential equations (2-30). Since, these equations are not explicitly a function of λ , the solution is theoretically valid for vanishingly small values of λ only. However, for a large class of practical problems, the radius ratio lies between $1/3$ and $1/2$, and occasionally it goes as high as 0.8 .

The solution herein presented is a generalization of the Clark and Reissner (8) solution, and reduces to theirs for $\lambda = 0$.

3.1 Series Expansion

Since the coefficients of the governing coupled differential equations appear as trigonometric functions, it is reasonable to assume the dependent variables, β and γ , in the form of trigonometric series.

Let the solution to (2-28) and (2-29) be:

$$\gamma = -\mu k s \left[\cos \phi + \sum_{n=2}^{\infty} B_{2n-1} \cos(2n-1)\phi \right]$$

$$\frac{d\beta}{d\phi} = \frac{\mu^2 k s}{4(1+\lambda \sin \phi)} \left[-\cos 2\phi \right. \tag{3-1}$$

$$\left. + \sum_{n=2}^{\infty} 2 B_{2n-1} \left(\frac{\cos 2(n-1)\phi}{2(n-1)} - \frac{\cos 2n\phi}{2n} \right) \right]$$

where B_{2n-1} represents coefficients yet to be determined.

Substituting equations (2-30) into (2-28), it is easily verified that the solution presented satisfies the equilibrium equation automatically for all values of λ . However, the equation of compatibility (2-29) is not automatically satisfied for all λ .

Also it may be observed that in the simple case where $\lambda = 0$, both equations (2-28) and (2-29) are satisfied; i. e., the present solution essentially reduces to that given by Clark and Reissner.⁽⁸⁾

3.2 Application of Theorem of Minimum Complementary Energy

Since the equations of equilibrium are satisfied by the proposed solution, the satisfaction of the compatibility condition will be insured by minimizing the total complementary energy: (12)

$$\delta V_c = \delta(U - W) = 0 \quad (3-2)$$

where U is the strain energy written in terms of the stresses and W , the potential energy of the end moments.

In a thin tube, the contribution of Q_ϕ and N_ϕ to the strain energy may be neglected, and κ_θ may be neglected in comparison to κ_ϕ , hence using (2-22), (2-33) becomes:

$$U = \frac{b}{2} \int \int \left[\frac{N_\theta^2}{Eh} + \frac{M_\phi^2}{D} \right] r \, d\phi \, d\theta \quad (3-3)$$

where the double integral extends over the entire middle surface of the tube.

Using (2-7), (2-19), (2-22) and (2-25), we may write (3-3) as

$$U = \frac{D}{2b} \int_{-\frac{\Theta_0}{2}}^{\frac{\Theta_0}{2}} \int_0^{2\pi} r \left[\left(\frac{d\alpha}{d\phi} \right)^2 + \left(\frac{d\beta}{d\phi} \right)^2 \right] d\phi d\theta \quad (3-4)$$

where Θ_0 represents the central angle of the bent tube.

The potential energy of the end moments is:

$$W = 2m \Delta \Big|_{\theta = \frac{\Theta_0}{2}}$$

or

$$W = m k \Theta_0 \quad (3-5)$$

where m is the applied moment. It is obvious $\delta W = 0$.

Thus

$$\delta V_c = \delta U = 0 \quad (3-6)$$

The minimum complementary energy can thus be conveniently obtained in the Rayleigh-Ritz manner by letting

$$\frac{\partial V_c}{\partial B_{2n-1}} = \frac{\partial U}{\partial B_{2n-1}} = 0 \quad (3-7)$$

which yields a system of N simultaneous, linear, algebraic equations in N unknowns, B_{2n-1} ; where $N = n - 1$ represents the number of arbitrary coefficients.

3.3 Stress Intensification and Rigidity Factors

The stress intensification factor may be defined as the ratio of the stress in a curved tube to that in an "equivalent" straight tube. An equivalent tube is one having the same moment of inertia, radius of cross section, and applied end moment as the curved tube. Thus, the stress intensification factors in the meridional and longitudinal directions become:

$$\begin{aligned}
 S_{\phi} &= \frac{\sigma_{\phi}}{mb/I} = \frac{I}{mb} \left[\frac{N_{\phi}}{h} + \frac{6M_{\phi}}{h^2} \right] \\
 &= \frac{E I h}{mb \sqrt{12(1-\nu^2)}} \left[\frac{\delta \cos \phi}{r} + \frac{6}{b \sqrt{12(1-\nu^2)}} \frac{d\beta}{d\phi} \right] \\
 S_{\theta} &= \frac{\sigma_{\theta}}{mb/I} = \frac{I}{mb} \left[\frac{N_{\theta}}{h} + \frac{6M_{\theta}}{h^2} \right] \quad (3-8) \\
 &= \frac{E I h}{mb \sqrt{12(1-\nu^2)}} \left[\frac{d\gamma}{b d\phi} + \frac{6\nu}{b \sqrt{12(1-\nu^2)}} \frac{d\beta}{d\phi} \right]
 \end{aligned}$$

where the positive sign pertains to the inner surface of the tube.

In order to satisfy equilibrium at any cross section, (2-20) must be satisfied. For thin-walled tubes, the second term of the integrand may be neglected in comparison with the first term; hence:

$$m = \int_0^{2\pi} N_{\theta} b r d\phi$$

Applying (2-17) and (2-25):

$$m = \frac{E h^2}{\sqrt{12(1-\nu^2)}} \int_0^{2\pi} r \frac{d\gamma}{d\phi} d\phi$$

Since:

$$\oint \frac{d(r\gamma)}{d\phi} d\phi = 0$$

the above equation may be written in the form:

$$m = - \frac{E h^2}{\sqrt{12(1-\nu^2)}} \int_0^{2\pi} \gamma \frac{dr}{d\phi} d\phi \quad (3-9)$$

Substituting (3-1) into (3-9) and integrating, one gets:

$$\begin{aligned} m &= \frac{E h^2 b}{\sqrt{12(1-\nu^2)}} \mu k S \pi \\ &= S E I \frac{k}{a} \end{aligned} \quad (3-10)$$

where I represents the moment of inertia of the tube, k/a represents the change in curvature of the tube centerline, $S E I$ is simply the effective rigidity of the tube, and S may be called the rigidity factor.

It is noted that the work done by the end moments is $1/2 W$, which must be stored in the tube as strain energy:

$$U = \frac{1}{2} W \quad (3-11)$$

The strain energy expression (3-4) may be written in the following condensed form:

$$U = \frac{D \Theta_0}{2 b} a \mu^2 k^2 S^2 \pi \Phi \quad (3-12)$$

where

$$\Phi = \frac{1}{a \mu^2 k^2 S^2 \pi} \int_0^{2\pi} r \left[\left(\frac{d\gamma}{d\phi} \right)^2 + \left(\frac{d\beta}{d\phi} \right)^2 \right] d\phi \quad (3-13)$$

Substituting (3-5), (3-10) and (3-12) into (3-11):

$$\frac{D \Theta_0}{2b} a \mu^2 R^2 S^2 \pi \Phi = \frac{1}{2} S E I \frac{R^2 \Theta_0}{a}$$

or, after simplification:

$$\Phi = \frac{1}{S} \quad (3-14)$$

since S is the rigidity factor, its inverse, Φ may be called the flexibility factor.

3.4 Evaluation of Integrals

A. Binomial Expansion

In applying the Theorem of Minimum Complementary Energy, integrals of the following type arise which require evaluation before the system of algebraic equations can be solved:

$$\int_0^{2\pi} \frac{\cos n\phi}{1 + \lambda \sin \phi} d\phi \quad (3-15)$$

One approximate method of determining the value of this integral is to expand the denominator using the binomial expansion. This is permissible, since λ is always less than unity. Thus:

$$\frac{1}{1 + \lambda \sin \phi} = 1 - \lambda \sin \phi + \lambda^2 \sin^2 \phi - \dots \quad (3-16)$$

Applying (3-11), there yields for $n = 2$:

$$\left[\frac{144}{\mu^2} + \frac{5}{4} + \frac{7\lambda^2}{8} \right] B_3 - \left[\frac{1}{4} + \frac{7\lambda^2}{24} \right] B_5 \\ + \frac{\lambda^2}{24} B_7 + \dots = 1 + \frac{5\lambda^2}{8}$$

and if $n = 3$, there results:

$$-\left[\frac{1}{4} + \frac{7\lambda^2}{24} \right] B_3 + \left[\frac{400}{\mu^2} + \frac{13}{36} + \frac{19\lambda^2}{72} \right] B_5 \\ - \left[\frac{1}{9} + \frac{17\lambda^2}{144} \right] B_7 + \dots = -\frac{\lambda^2}{16}$$

and so on. The undetermined coefficient can then be solved in terms of μ and λ .

The flexibility factor becomes:

$$\Phi = 1 + \frac{\mu^2}{16} - \frac{\mu^2}{8} B_3 \\ + \sum_{n=2}^{\infty} B_{2n-1}^2 \left[(2n-1)^2 + \frac{\mu^2}{16} \left(\frac{1}{n^2} + \frac{1}{(n-1)^2} \right) \right] \\ - \frac{\mu^2}{8} \sum_{n=2}^{\infty} B_{2n-1} B_{2n+1} \frac{1}{n^2} \\ + \frac{\mu^2 \lambda^2}{32} \left[1 - \frac{5}{2} B_3 + \frac{1}{4} B_5 \right. \\ \left. + \sum_{n=2}^{\infty} B_{2n-1}^2 \left(\frac{1}{n^2} + \frac{1}{(n-1)^2} + \frac{1}{n(n-1)} \right) \right. \\ \left. - \sum_{n=2}^{\infty} B_{2n-1} B_{2n+1} \left(\frac{1}{(n-1)n} + \frac{1}{n(n+1)} + \frac{2}{n^2} \right) \right. \\ \left. + \sum_{n=2}^{\infty} B_{2n-1} B_{2n+3} \frac{1}{n(n+1)} \right] + O(\lambda^4)$$

B. Exact Integral

Instead of expanding the integrand in (3-15) using the binomial expansion, the general solution can be improved by using the closed-form solution for the definite integrals. One notes:

$$\int_0^{2\pi} \frac{\cos n\phi}{1+\lambda \sin \phi} d\phi = \operatorname{Re} \int_0^{2\pi} \frac{e^{in\phi} d\phi}{1+\lambda \sin \phi} = \operatorname{Re} \oint \frac{z^n dz}{iz \left[1 + \frac{\lambda(z^2-1)}{2iz} \right]}$$

where

$$e^{in\phi} = z^n$$

$$d\phi = \frac{dz}{iz}$$

$$1 + \lambda \sin \phi = 1 + \frac{\lambda(z^2-1)}{2iz}$$

The above integral may be rewritten as:

$$\frac{2}{\lambda} \oint \frac{z^n dz}{(z-c)(z-d)}$$

with poles at points:

$$c = \frac{i}{\lambda} (\sqrt{1-\lambda^2} - 1) \quad , \quad d = -\frac{i}{\lambda} (\sqrt{1-\lambda^2} + 1)$$

It is noted that d is outside of the unit circle, and the integral is simply:

$$\begin{aligned} \int \frac{e^{in\phi} d\phi}{1+\lambda \sin \phi} &= 2\pi i \operatorname{Res}(c) = \frac{4\pi i}{\lambda} \frac{c^n}{(c-d)} \\ &= 2\pi \cdot c^n / \sqrt{1-\lambda^2} \end{aligned}$$

It follows then:

$$\int_0^{2\pi} \frac{\cos n\phi}{1+\lambda \sin \phi} d\phi = 2\pi C^n / \sqrt{1-\lambda^2} \quad : n \text{ even} \quad (3-17)a$$

$$= 0 \quad : n \text{ odd}$$

$$\int_0^{2\pi} \frac{\sin n\phi}{1+\lambda \sin \phi} d\phi = 2\pi C^n / \sqrt{1-\lambda^2} \quad : n \text{ odd} \quad (3-17)b$$

$$= 0 \quad : n \text{ even}$$

For this case, Φ in (3-14) takes the form:

$$\Phi = \sum_{n=1}^{\infty} B_{2n-1}^2 (2n-1)^2 + \frac{\mu^2}{16} \left[\sum_{n=1}^{\infty} B_{2n-1}^2 G_{nn} + 2 \sum_{n=1}^{\infty} \sum_{m=n+1}^{\infty} B_{2n-1} B_{2m-1} G_{nm} \right]$$

In the above equation, B_1 is taken to be unity, but the remaining coefficients B_{2n-1} are yet to be determined. The functions G_{nm} are defined as follows:

$$G_{nm} = \frac{1}{\pi} \int \left[\frac{\cos 2n\phi}{n} - \frac{\cos 2(n-1)\phi}{n-1} \right] \left[\frac{\cos 2m\phi}{m} - \frac{\cos 2(m-1)\phi}{m-1} \right] \frac{d\phi}{r}$$

$$G_{1,m} = \frac{1}{\pi} \int \cos 2\phi \left[\frac{\cos 2m\phi}{m} - \frac{\cos 2(m-1)\phi}{m-1} \right] \frac{d\phi}{r} \quad (3-18)$$

$$G_{1,1} = \frac{1}{\pi} \int \frac{\cos^2 2\phi}{1+\lambda \sin \phi} d\phi$$

By using trigonometric identities, the integrals in (3-18) can be decomposed into several integrals for which closed-form solutions are given above. The minimization of the complementary energy will result in a set of simultaneous equations in terms of λ and μ from which the undetermined coefficients are obtained.

3.5 Discussion of Results

To evaluate the analytical methods, published experimental results are presented in Figure 2 for ρ , and Figures 3-6 for stress distribution. The analytical results are obtained by using the binomial expansion to order of λ^4 . In Figure 2, the experimental data obtained by Gross and Ford⁽⁵⁾ confirm very well the theoretical prediction. On the other hand, data points obtained by Vissat and DelBuono⁽⁷⁾ are consistently higher than the theory predicts. These high experimental values are believed to be due essentially to end restraints attendant to load application on a short radius bend.

In Figures 3 and 4, the theoretical stress distributions as predicted by the general solution using the binomial expansion are plotted against the experimental data for λ around one-third obtained by Gross and Ford⁽⁵⁾. Similarly, in Figures 5 and 6, the theoretical stress distributions are presented with the experimental data for λ around one-half obtained by Vissat and Del Buono⁽⁷⁾. The theoretical predictions seem to be confirmed well by experimental results.

In computing the rigidity and the stress intensification factor using either the binomial expansion or the closed-form for the integrals, the solution is found to be always rapidly convergent. Depending on the magnitude of μ and also to a lesser extent on that of λ , taking four to six terms in the series solution is always adequate.

The rigidity factor, ξ , as computed using the binomial expansion and the closed form integral solution are given in Figures 2 and 2A, respectively. They are presented as a function of μ and λ . The fact that the curves deviate from each other at large pipe parameter indicates that ξ is sensitive to the truncation of higher order terms in the binomial expansion at large values of μ . On the other hand, the stress distribution and the peak value of stress is rather insensitive to such truncation. As a result, both approaches give almost identical peak stress and only a slight change in stress distribution.

It is noted in Figure 2A that the effect of λ on the rigidity factor, ξ , is minor and diminishes with increasing μ . In fact at μ beyond 100, none of the three curves is distinguishable from the asymptotic formula $\xi = \frac{1}{2} \left(\frac{1}{\mu} + \frac{1}{\lambda} \right)$. Thus, as far as the rigidity factor is concerned, the present results confirm what has been found by other investigators $\xi = \frac{1}{2} \left(\frac{1}{\mu} + \frac{1}{\lambda} \right)$.

The effect of μ and λ on the meridional stress intensification factor can be seen in Figures 7 and 8 for $\mu = 100$ and 16.5, respectively. It should be noted that λ not only affects the peak stress, but it also influences substantially the stress distribution in the inner half of the tube. Further, at large μ , the peak meridional stress always occurs at $\phi = 0$; but, at moderate μ , increasing

λ tends to shift the location of maximum stress toward the intrados. Similar figures were obtained for the longitudinal stress intensification factor, but the peak value is always smaller than that in the meridional direction, and hence are not presented.

Usually one is less interested in the stress distribution around the pipe bore, than in the peak stress intensification factor, which always occurs at the inner surface. The peak stress is presented in Figure 9. All the curves are terminated at the lower limit of μ at which the thin shell assumption is still considered valid. Also shown, in dotted line, are the asymptotic solutions ⁽⁸⁾⁽⁹⁾ which are valid for $\lambda = 0$ and large μ . As expected, the asymptotic solution coincides with the curve for $\lambda = 1/10$ at large μ , and deviates from the results of the general solution at the lower range of μ . But the effect of λ on the peak stress intensification factor, particularly in the range of practical interest, is by no means negligible. Hence for λ different from zero, the existing asymptotic formulas ⁽⁸⁾⁽⁹⁾ must be re-examined. This is carried out in Chapter 4.

The analytical results of the general solution are rapidly convergent. The required number of terms in the series expansion seems to depend largely on the value of μ . For the meridional stress, which is the least convergent of all the quantities of interest, only four

terms are required for μ around 20, and six terms are sufficient for μ as large as 100. In the latter case, only a 6x6 matrix is required. The coefficients of B_{2n-1} , decrease at least three orders of magnitude in these cases.

To illustrate the advantage of the present method over existing ones, it should be pertinent to make some comparison. The present method requires solving a 4x4 matrix for $\mu \doteq 46$. Tueda's method ⁽¹⁾ requires complicated numerical computations and solving a 20x20 matrix for $\mu \doteq 37$. No converging results can be obtained by solving even a much larger matrix for $\mu \doteq 46$. In fact, his results are not convergent at $\lambda \geq \frac{1}{2}$ for any value of μ . The method of ⁽³⁾ Turner and Ford involves straightforward numerical computations, but it requires a solution of a 25x25 matrix in the case of $\mu \doteq 37$ and of a 49x49 matrix in the case of $\mu \doteq 46$. The cosine series solution ⁽⁴⁾ proposed by Jones requires a 10x10 matrix for $\mu \doteq 46$ whereas ⁽²⁾ the method proposed by Symonds and Pardue requires only a six-term expansion. However, like Jones, they made the assumption that the meridional middle surface is inextensible. As a consequence, the meridional stresses in the inner and outer surfaces of the tube are always equal and opposite. This was found to be unrealistic and to ⁽⁵⁾ err on the unconservative side.

CHAPTER 4

ASYMPTOTIC SOLUTION FOR AXISYMMETRIC CASE

For large μ , a solution for the axisymmetric case, by asymptotically integrating the governing differential equations becomes very attractive. The formulas for the rigidity and maximum stress intensification factors, in this upper range of μ , reduce to relatively simple and concise expressions thus making them exceptionally useful.

As it was pointed out in the previous chapter the effect of λ on the peak stress intensification factor, particularly in the range of practical interest, is by no means negligible. So far, asymptotic solution exists only for the case $\lambda = 0$ or vanishingly small λ . If λ is substantially different from zero, the existing asymptotic formulas (8) must be modified to reflect its effect.

4.1 Theory and Solution

Combining (2-28) & (2-29) and writing these in complex form:

$$\frac{d^2 z}{d\phi^2} + \frac{\lambda \cos \phi}{1 + \lambda \sin \phi} \frac{dz}{d\phi} - i\mu \frac{\sin \phi}{1 + \lambda \sin \phi} z = i\mu \frac{R \cos \phi}{1 + \lambda \sin \phi} \quad (4-1)$$

where

$$z = \beta + i\gamma \quad (4-2)$$

It is noted that for thin tubes, $\lambda \ll \mu$. For very large value of μ ,

(4-1) may be simplified to:

$$\frac{d^2 z}{d\phi^2} - i\mu \frac{\sin\phi}{1+\lambda\sin\phi} z = i\mu k \frac{\cos\phi}{1+\lambda\sin\phi} \quad (4-3)$$

For large μ , the general solution, discussed previously, indicates that the peak stress always occurs in the meridional direction and near $\phi = 0$. In the neighborhood of $\phi = 0$, (4-3) reduces to:

$$\frac{d^2 z}{d\phi^2} - i\mu\phi z = i\mu k \quad (4-4)$$

Using the following transformation to stretch the variables:

$$x = \mu^{1/3} \phi \quad (4-5)$$

$$T(x) = \frac{z}{ik\mu^{1/3}}$$

The differential equation (4-4) reduces to the form:

$$\frac{d^2 T}{dx^2} - i x T = 1 \quad (4-6)$$

where

$$T(x) = T_r(x) + i T_i(x) \quad (4-7)$$

The subscripts r and i stand for real and imaginary, respectively.

Substituting (4-5) and (4-7) into (4-2):

$$\begin{aligned}\alpha &= \mu^{1/3} k T_r(x) \\ \beta &= -\mu^{1/3} k T_i(x)\end{aligned}\tag{4-8}$$

and the initial conditions which are obtained from the general solution for large μ :

$$\begin{aligned}\beta(0) &= 0 \\ \frac{d\alpha(0)}{d\phi} &= 0\end{aligned}\tag{4-9}$$

are satisfied if:

$$\begin{aligned}T_i(0) &= 0 \\ \frac{dT_r(0)}{dX} &= 0\end{aligned}\tag{4-10}$$

The initial conditions in (4-9) are obviously justified by the results obtained from the general solution as discussed earlier.
(8)

A solution to (4-6) was given by Clark and Reissner in terms of Lommel functions for the case of $\lambda = 0$.

Alternatively, the differential equation may be solved by numerical integration techniques, such as Runge-Kutta, provided the additional conditions are specified:

$$\begin{aligned}T_r(0) &= -1.2879 \\ \frac{dT_i(0)}{dX} &= 0.9389\end{aligned}\tag{4-11}$$

These conditions are obtained from the Lommel function at $x = 0$. (10)

The maximum stresses are known to occur near $\phi = 0$.

Thus, using the approximation $\sin\phi \doteq \phi$ and $\cos\phi \doteq 1$, one obtains from (3-8), using (4-8):

$$S_{\phi} = \frac{\mu^{2/3}}{2} \left[\frac{\lambda}{\mu^{1/3}} T_r + \sqrt{\frac{3}{1-\nu^2}} \frac{dT_i}{dx} \right] \quad (4-12)$$

$$S_{\theta} = \frac{\mu^{2/3}}{2} \left[\frac{dT_r}{dx} + \nu \sqrt{\frac{3}{1-\nu^2}} \frac{dT_i}{dx} \right]$$

and

$$S_{\phi} - S_{\theta} = \frac{\mu^{2/3}}{2} \left[\frac{\lambda}{\mu^{1/3}} T_r - \frac{dT_r}{dx} + \sqrt{\frac{3(1-\nu)}{1+\nu}} \frac{dT_i}{dx} \right]$$

in which the top sign refers to the inner surface of the tube.

4.2 Discussion of Results

In (4-12), the maximum absolute values for $T_r(x)$ and $\frac{dT_i(x)}{dx}$ happen to be their initial values. Hence, S_{ϕ} is maximum at $\phi = 0$ and its magnitude is dependent on both μ and λ . In the practical range of μ and λ , the contribution of the direct stress (first term) is not necessarily negligible as seen in Figure 9. The curves representing the general solution merge with the asymptotic solution at large μ ; but these curves are still distinct for different λ . It is found that except for very small values of μ and λ , S_{ϕ} is always more critical than S_{θ} or $S_{\phi} - S_{\theta}$ and hence the latter two expressions are not plotted. Therefore, for $\nu = 0.3$, a compact expression

for the peak stress in a tube is obtained from (4-12) as follows:

$$|S_{\phi}|_{\max.} = 0.86\mu^{2/3} \left[0.75 \frac{\lambda}{\mu^{1/3}} + 1 \right] \quad (4-13)$$

Comparing with the results shown in Figure 9, (4-13) traces exactly the curves obtained by the general solution for each λ , except for $\lambda = 0.1$ at values of μ below, say 10. Obviously the asymptotic formula should no longer be valid for such small values of μ .

(9)

Clark pointed out that the asymptotic solutions given in Reference 8 represent only the leading terms of the asymptotic expansions. By retaining the next higher order term, he obtained the following peak stress intensification factor:

$$|S_{\phi}|_{\max.} = 0.86\mu^{2/3} - 0.278 \quad (4-14)$$

It is noted that λ is absent from (4-14), hence it is valid only for

$\lambda = 0$. By plotting (4-14) on Figure 9, an excellent agreement with the results for $\lambda = 0.1$ obtained by the general solution is seen, as long as μ is not too small.

Experimental results are presented along with the asymptotic solutions in Figure 10. Except for the results reported by Gross and Ford⁽⁵⁾, most of the available data are obtained by using strain gages only on the outer surface⁽⁶⁾⁽⁷⁾. It is noted that the results

(6)
by Pardue and Vigness are excellent, while the results of Vissat and
(7) (5)
Del Buono are consistently low. The results by Gross and Ford
are also very good. The difference between the absolute value of the
stress on the inner and outer surfaces indicates the contribution of the
meridional membrane stress.

It should be pointed out that most of the data reported by
(7)
Vissat and Del Buono are obtained from tubes with the thickness-
radius ratio substantially in excess of 1/10 which means relatively
thick tubes. On the other hand, it is interesting to see that the data for
 $\lambda = 1/2$ is also consistently lower than those for $\lambda = 1/3$ which con-
forms to the trend of the theoretical prediction.

CHAPTER 5

ASYMMETRIC CASE

Apparently, there has been no solution published for the in-plane bending of a thin-walled tube having rigid end flanges. Because of the flanges, the solution will no longer be independent of the longitudinal coordinate, Θ , as was the case for the axisymmetric solutions presented in Chapters 3 and 4. Theoretical investigations, to date, have been solely concerned with the relatively simple case of axisymmetric bending; although some experimental data⁽⁶⁾ is available for tubes with flanges.

The end flanges have the effect of reducing the ovalization of cross sections in the vicinity of the ends. This decrease in ovalization will tend to reduce the flexibility and peak meridional stress. The peak longitudinal stress is expected to increase as cross sectional distortion is reduced.

Of course, the extent of distortion will depend primarily on two parameters, Θ_0 and μ . As Θ_0 decreases, the effect of the flanges will be felt over an increasingly larger proportion of the tube, and, the effect of shear should start to be of comparable magnitude to the bending and normal stresses. The inclusion of all the above effects would make the problem quite complicated. Further, the existing experimental data⁽⁶⁾ for Θ_0 less than 180° is erratic.

In this chapter, a solution will be presented for a U-bend ($\Theta_0 = \pi$) for which reasonable experimental data are available. In what follows, a solution will be proposed in which the displacements are expanded in trigonometric series in such a manner that would satisfy the compatibility conditions, and the total potential energy will be minimized in the Rayleigh-Ritz manner to insure satisfaction of the equilibrium equations.

In the formulation of the problem, the usual assumptions will be made, namely:

- a) Plane sections remain plane
- b) Inextensible meridional centerline
- c) Shear contribution negligible

The assumption imposing the inextensibility of the meridional centerline is not strictly true except in the vicinity of the end flanges. However, the general theory for an axisymmetric tube indicates that this assumption does not seriously affect the axisymmetric results and should affect to an even smaller extent the results for the asymmetric case since the flanges hinder ovalization.

The assumption which neglects the contribution of the shear strain in comparison with the bending strain is considered justifiable

for a U-bend, since, the effect of the rigid flanges is expected to decay rapidly away from the ends.

5.1 Displacements

Following the assumption of the inextensibility of the middle surface in the meridional direction, i. e., $\epsilon_{\phi_0} = 0$, one obtains:

$$w_{\phi} = -\frac{R\phi}{b} \frac{\partial w_{\phi}}{\partial \phi} \quad (5-1)$$

It should be noticed that this assumption reduces the number of displacements which must be expanded in series form.

Further, from the assumption that plane cross sections remain plane, one may write:

$$w_{\theta} = q + (b \sin \phi) \Delta \quad (5-2)$$

where q represents the extension of the centerline of the tube, and Δ the rotation of the cross-section. Obviously, in this asymmetric case, Δ should be a function of θ .

To satisfy the symmetry conditions for w_{ϕ} and w_{θ} , the displacement in the meridional direction may be expanded in the form:

$$\begin{aligned} \omega_{\phi} = & \sum_{s=1,3}^{M8} \left[\sum_{t=1,3}^{M8} \omega_{ts} \cos t\phi \right. \\ & \left. + \sum_{t=2,4}^{M8} \omega_{ts} \sin t\phi \right] \cos \frac{s\pi\theta}{\theta_0} \end{aligned} \quad (5-3)$$

Similarly, from symmetry conditions, Δ may be expanded as an odd function in θ , namely:

$$\Delta = b_0 \theta + \sum_{n=1}^{M8} b_n \frac{\theta_0}{n\pi} \sin \frac{n\pi\theta}{\theta_0} \quad (5-4)$$

5.2 Application of Theorem of Minimum Potential Energy

The expression for the total potential energy, neglecting the shear strain, is given by (2-33). Considering the manner in which the tube ovalizes, one would expect the change in curvature in the meridional direction to be much greater than the curvature change in the longitudinal direction. This should be true over a major portion of the tube, except in the immediate vicinity of the end flanges where K_{ϕ} vanishes. In conformity with the above assumption, as well as the inextensibility of the meridional centerline, (2-33) simplifies to the following form:

$$U = \frac{1}{2} \int \int [C \epsilon_{\theta_0}^2 + D K_{\phi}^2] b r d\phi d\theta \quad (5-5)$$

Substituting (2-5) and (2-7) into (5-5), one obtains:

$$\begin{aligned}
 U = \frac{C}{2} \int \int \left[\frac{1}{r} \frac{\partial w_\theta}{\partial \theta} + \frac{w_\theta}{br} \frac{\partial r}{\partial \phi} + \frac{w_\theta}{R_\theta} \right]^2 br d\phi d\theta \\
 + \frac{D}{2} \int \int \left[\frac{1}{b} \left(-\frac{1}{b} \frac{\partial^2 w_\theta}{\partial \phi^2} + \frac{1}{R_\phi} \frac{\partial w_\theta}{\partial \phi} \right) \right]^2 br d\phi d\theta \quad (5-6)
 \end{aligned}$$

where w_θ is given by (5-1).

The potential energy of the applied end moments is:

$$W = 2m\Delta \Big|_{\theta = \frac{\theta_0}{2}} \quad (5-7)$$

To insure that the equilibrium conditions are satisfied, the total potential energy will be minimized in the manner of Rayleigh-Ritz as follows:

$$\frac{\partial V_P}{\partial \omega_{\theta P}} = 0 \quad ; \quad \frac{\partial V_P}{\partial b_P} = 0 \quad ; \quad \frac{\partial V_P}{\partial \eta} = 0 \quad (5-8)$$

where

$$V_P = U - W$$

and

$$\eta \equiv \frac{a}{b} \quad ; \quad \omega_{\theta P} = -\frac{w_{\theta P}}{b}$$

The set of equations characterized by (5-8) may be written in the following form:

$$\frac{\partial V_P}{\partial \omega_{qP}} = 0 \quad \text{which gives:}$$

$$\sum_t^{\text{odd}} \sum_s^{\text{odd}} \omega_{ts} \left[\overline{\alpha_t \alpha_q} + \frac{P^2}{12} (t^3 - t)(q^3 - q) \pi \delta_{tq} \right] K_{SP}$$

$$+ \sum_t^{\text{even}} \sum_s^{\text{odd}} \omega_{ts} \left[\overline{\beta_t \alpha_q} - \frac{\lambda P^2}{12} (t^3 - t)(q^3 - q) C_{qt} \right] K_{SP}$$

$$- b_0 \overline{\alpha \sin q} L_P - \sum_n b_n \overline{\alpha \sin q} K_{np} - \eta \overline{\alpha q} L_P = 0$$

For q odd

$$\sum_t^{\text{odd}} \sum_s^{\text{odd}} \omega_{ts} \left[\overline{\alpha_t \beta_q} - \frac{\lambda P^2}{12} (t^3 - t)(q^3 - q) C_{tq} \right] K_{SP}$$

$$+ \sum_t^{\text{even}} \sum_s^{\text{odd}} \omega_{ts} \left[\overline{\beta_t \beta_q} + \frac{P^2}{12} (t^3 - t)(q^3 - q) \pi \delta_{tq} \right] K_{SP}$$

$$- b_0 \overline{\beta \sin q} L_P - \sum_n b_n \overline{\beta \sin q} K_{np} - \eta \overline{\beta q} L_P = 0$$

For q even

$$\frac{\partial V_P}{\partial b_0} = 0 \quad \text{which gives:}$$

$$\sum_t^{\text{odd}} \sum_s^{\text{odd}} \omega_{ts} \overline{\alpha \sin t} L_s - \sum_t^{\text{even}} \sum_s^{\text{odd}} \omega_{ts} \overline{\beta \sin t} L_s$$

$$+ b_0 I_2 \frac{\Theta_0}{2} + \sum_n b_n I_2 L_n + \eta I_1 \frac{\Theta_0}{2} = \frac{m \Theta_0 a \pi (1 - \nu^2)}{2EI}$$

$$\frac{\partial V_P}{\partial b_P} = 0 \quad \text{which gives:}$$

$$-\sum_t^{\text{odd}} \sum_s^{\text{odd}} \omega_{ts} \overline{\alpha \Delta \ln_t} E_{Ps} - \sum_t^{\text{even}} \sum_s^{\text{odd}} \omega_{ts} \overline{\beta \sin_t} E_{Ps} \\ + b_0 I_2 L_P + \sum_n b_n I_2 K_{nP} + \eta I_1 L_P = \frac{m \Theta_0 \alpha (1-\nu^2)}{E I P} \sin \frac{P\pi}{2}$$

$$\frac{\partial V_P}{\partial \eta} = 0 \quad \text{which gives:}$$

$$-\sum_t^{\text{odd}} \sum_s^{\text{odd}} \omega_{ts} \overline{\alpha_t} L_s - \sum_t^{\text{even}} \sum_s^{\text{odd}} \omega_{ts} \overline{\beta_t} L_s \\ + b_0 I_1 \frac{\Theta_0}{2} + \sum_n b_n I_1 L_n + \eta I_0 \frac{\Theta_0}{2} = 0$$

where

$$\overline{\alpha_g} = \oint \frac{\alpha_g d\phi}{1 + \lambda \sin \phi}$$

$$j \overline{\beta_g} = \oint \frac{\beta_g d\phi}{1 + \lambda \sin \phi}$$

$$\overline{\alpha_g \beta_t} = \oint \frac{\alpha_g \beta_t d\phi}{1 + \lambda \sin \phi}$$

$$I_0 = \oint \frac{d\phi}{1 + \lambda \sin \phi}$$

$$I_1 = \oint \frac{\sin \phi d\phi}{1 + \lambda \sin \phi}$$

$$I_2 = \oint \frac{\sin^2 \phi d\phi}{1 + \lambda \sin \phi}$$

$$L_n = \int_0^{\Theta_0/2} \cos \frac{n\pi\theta}{\Theta_0} d\theta$$

$$K_{Ps} = \int_0^{\Theta_0/2} \cos \frac{P\pi\theta}{\Theta_0} \cos \frac{s\pi\theta}{\Theta_0} d\theta$$

$$C_{tg} = \oint \sin t\phi \cos g\phi \sin \phi d\phi$$

and:

$$\alpha_t = \cos t\phi \cos \phi + t \sin t\phi \sin \phi$$

$$\beta_t = \sin t\phi \cos \phi - t \cos t\phi \sin \phi$$

$$\delta_{tq} - \text{Kronecker delta}$$

5.3 Discussion of Results

The coefficients of the series (5-3)(5-4) were observed to converge at a moderate rate. For relatively small values of μ (8.3), the ω_{ts} coefficients decrease two-orders in magnitude in the second subscript (Θ - direction) in 15 terms, and, five-orders in magnitude in the first subscript (ϕ - direction) in 8-terms. For relatively large values of μ (82.6), the ω_{ts} coefficients decrease three-orders in magnitude in the Θ - direction in 15-terms but only one and one-half orders in magnitude in the ϕ - direction in 8 terms. Thus, the ω_{ts} series is highly sensitive to truncation in the ϕ - direction and less sensitive in the Θ - direction at large values of μ .

For all μ , the b_n coefficients decrease monotonically one and one-half orders in magnitude in 15-terms while alternating in sign.

Although the series of coefficients is slowly convergent, the series defining the angular rotation, Δ , converges so well that four terms was found adequate. For all values of μ , the fourth through fifteenth terms in the series affected the total angular rotation of the ends of the tube by only 5%. The largest matrix solved was 135 x 135.

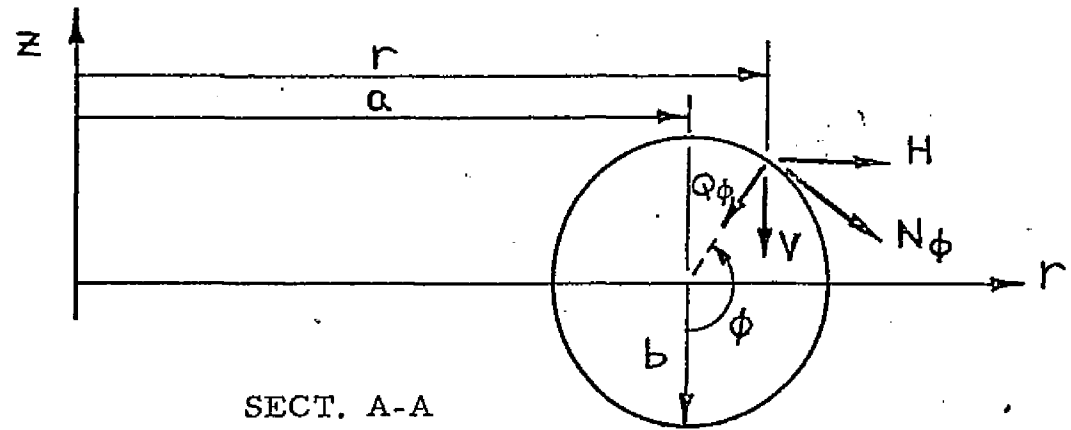
The flexibility factor was found to be the least sensitive to truncation of the series. The plot of flexibility factor, Φ , vs. pipe parameter, μ , Figure 11, shows that the theory herein presented appears to be an upper bound on the experimental data.

To explain the experimental data plotted on Figure 11, one may quote the authors, Pardue and Vigness⁽⁶⁾: "The range of flexibility factors, measured for a given bend length and end constraint was found to be approximately the same for in-plane and out-of-plane bending. Therefore, data for the three moments have been averaged for each bend length and end constraint, and plotted in Figure 11. Maximum and minimum values are shown by the extremities of the vertical line. Thus, the length of the line represents the range of flexibility factors caused by different types of loads for one combination of bend length and end constraint".

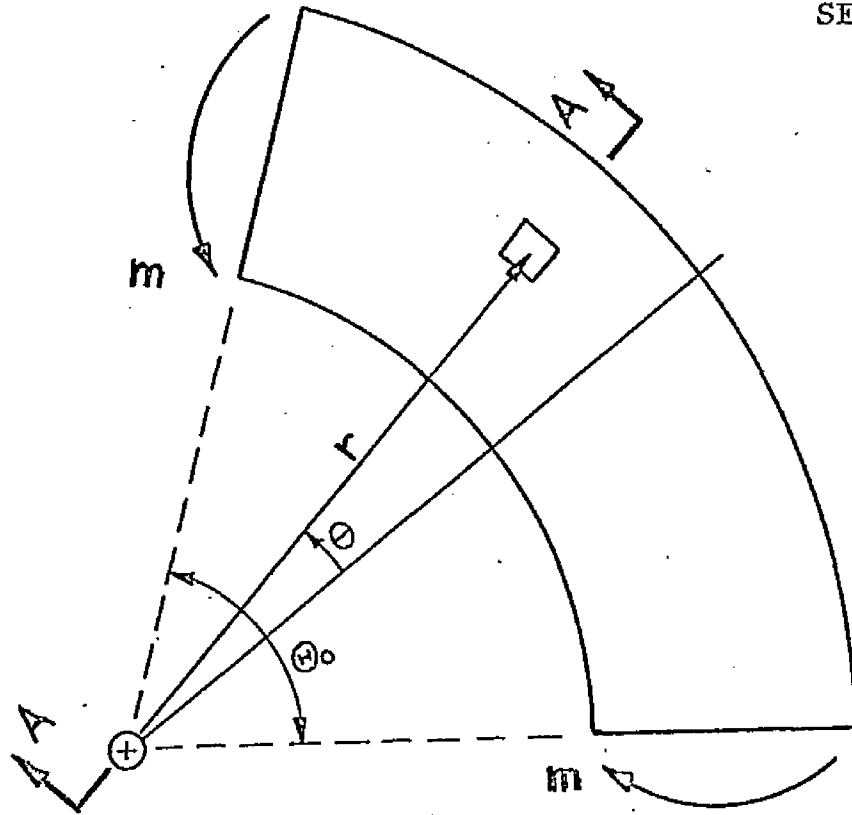
Of the two stress intensification factors, S_{ϕ} and S_{θ} , S_{ϕ} is seen always to be the greater, both experimentally and as predicted by the present theory (See Figures 12 and 13). As seen in Figure 12, the present theory is confirmed very well by the experimental data for the meridional stress intensification factor at large values of μ . It further appears to be an upper bound on the experimental results for this critical stress, S_{ϕ} . On the other hand, the experimental data for S_{θ} confirms rather well the analytical results.

As explained previously, attention was restricted to U shaped tubes of moderate to large values of μ , since the shear effect for these tubes could be considered negligible or at most its effect limited to a small portion of the tube near the end flanges. For tubes having a central angle of 90° or less, the shear effect should be increasingly more pronounced and significant. But, due to experimental difficulties, the available experimental data seems quite erratic for bends of 90° or less containing end flanges.

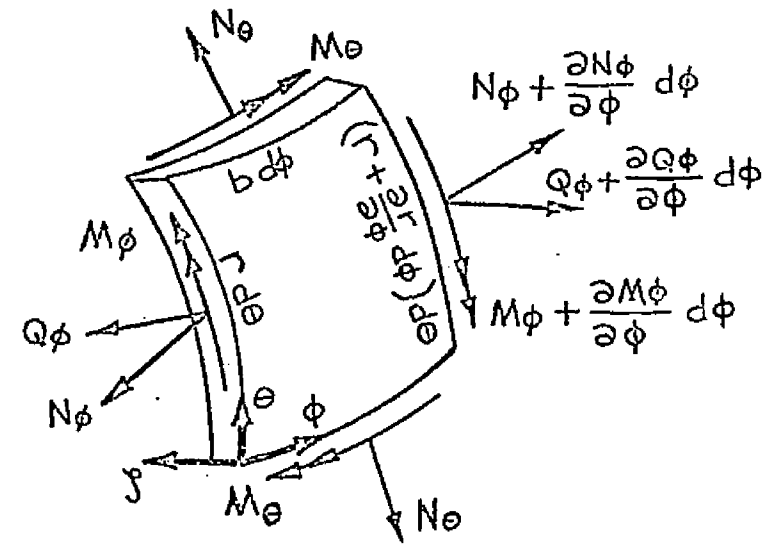
In summary, the analytical results for a U-bend with rigid end flanges seem to be reasonably confirmed by experiments. The assumptions used seem to be justifiable. Further refinement may be possible when larger matrices are used in conjunction with the deletion of some of the restrictions imposed.



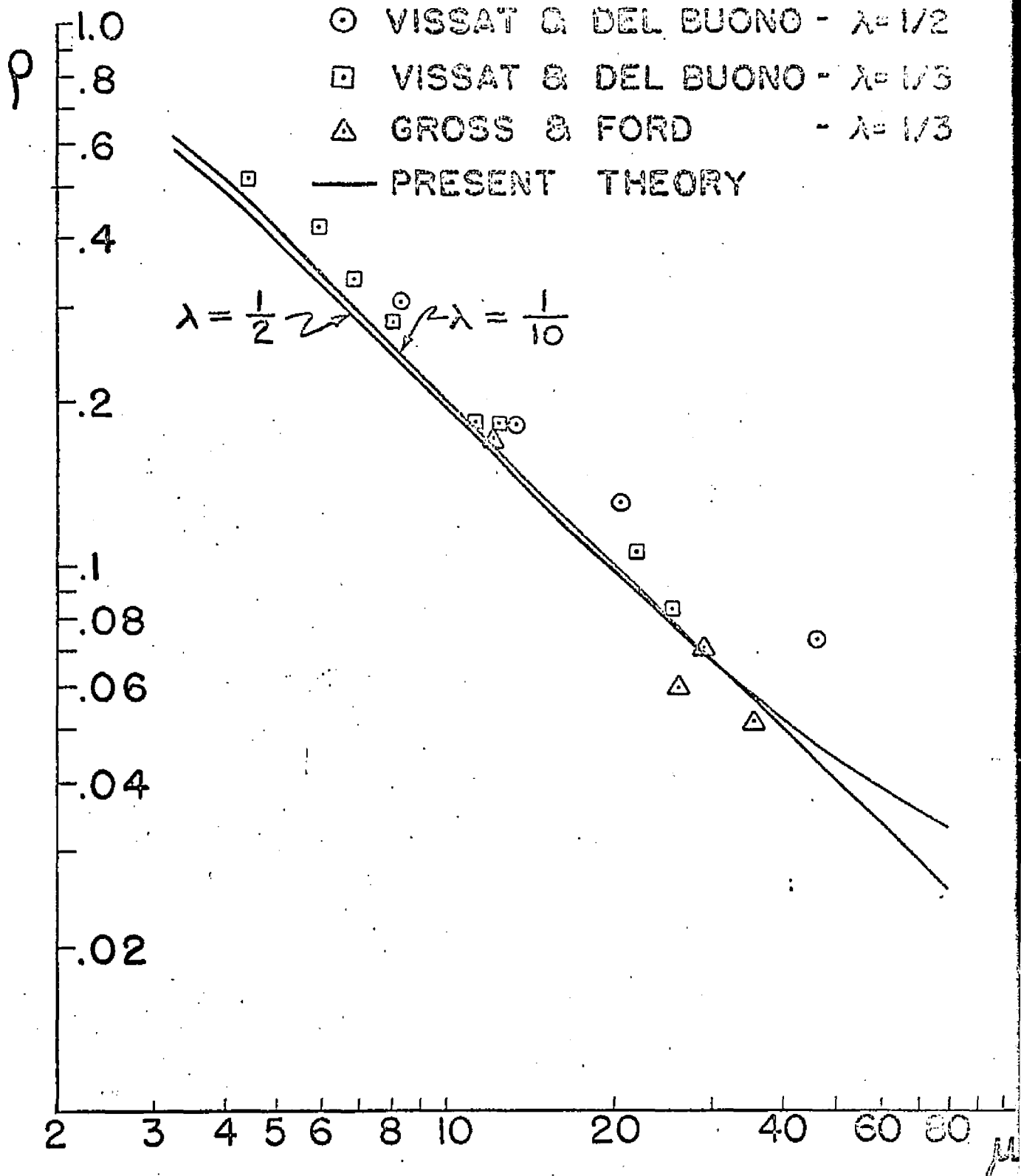
SECT. A-A



CURVED CIRCULAR TUBE
FIGURE 1



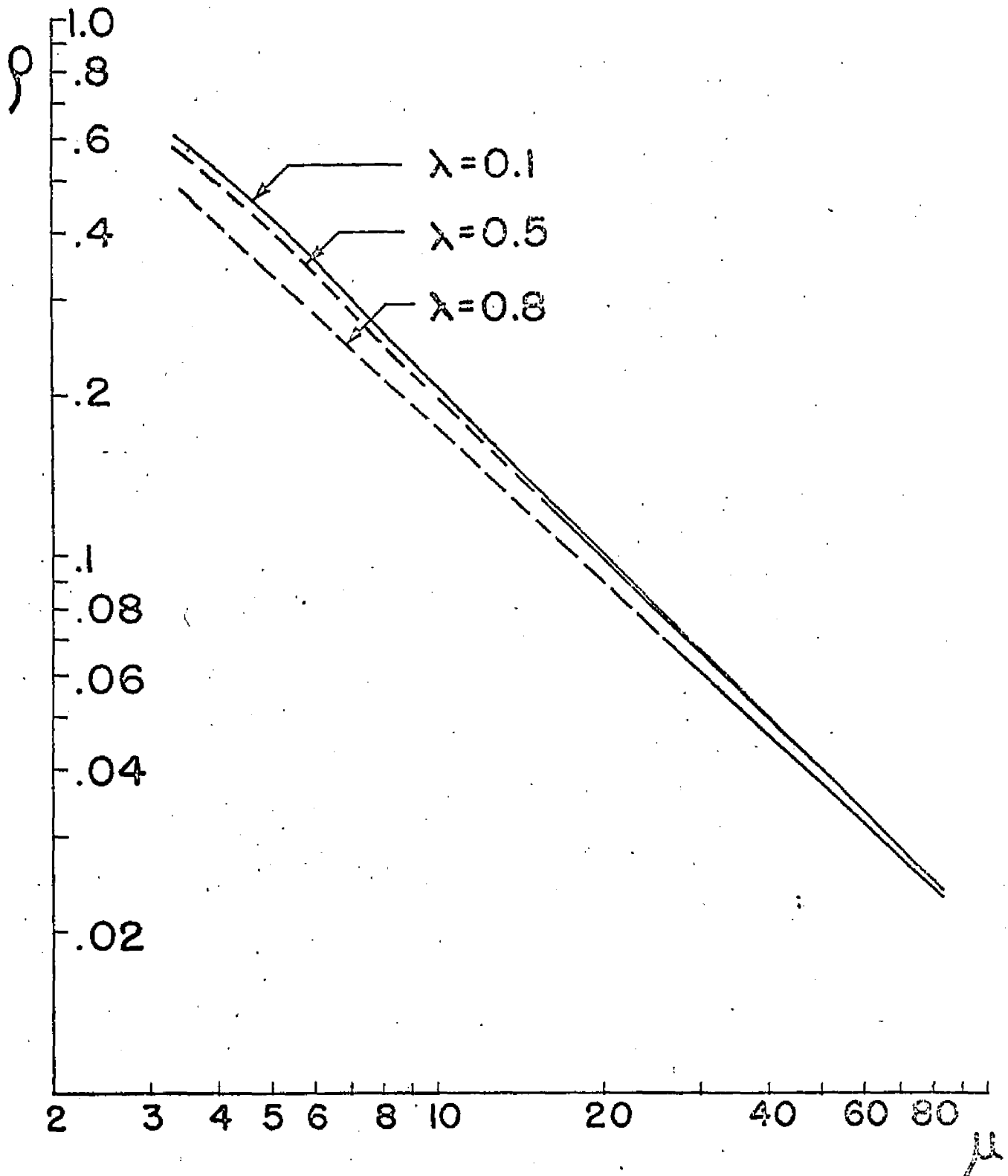
STRESSES ON AN ELEMENT



RIGIDITY FACTOR

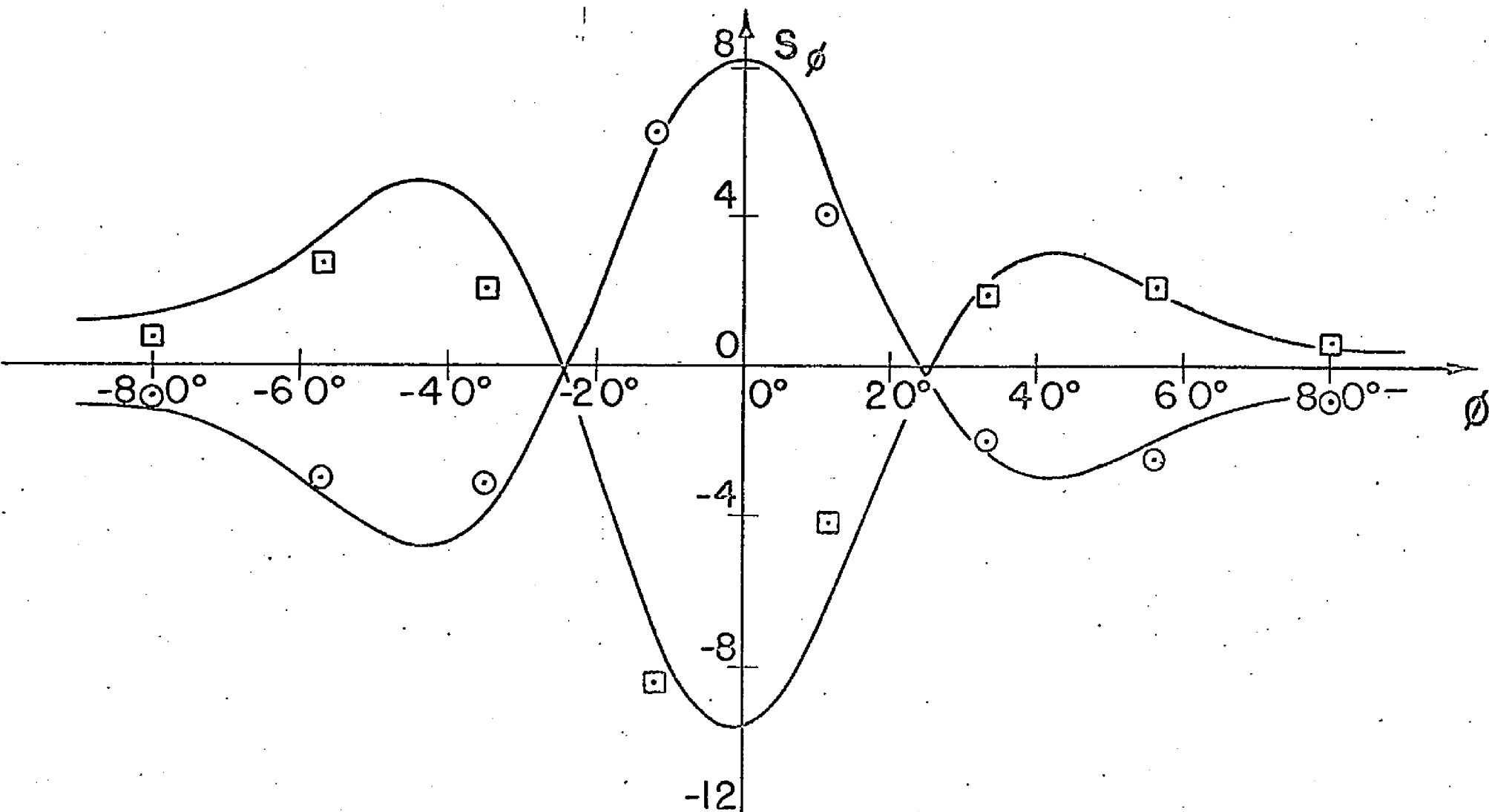
μ

FIGURE 2



RIGIDITY FACTOR vs μ

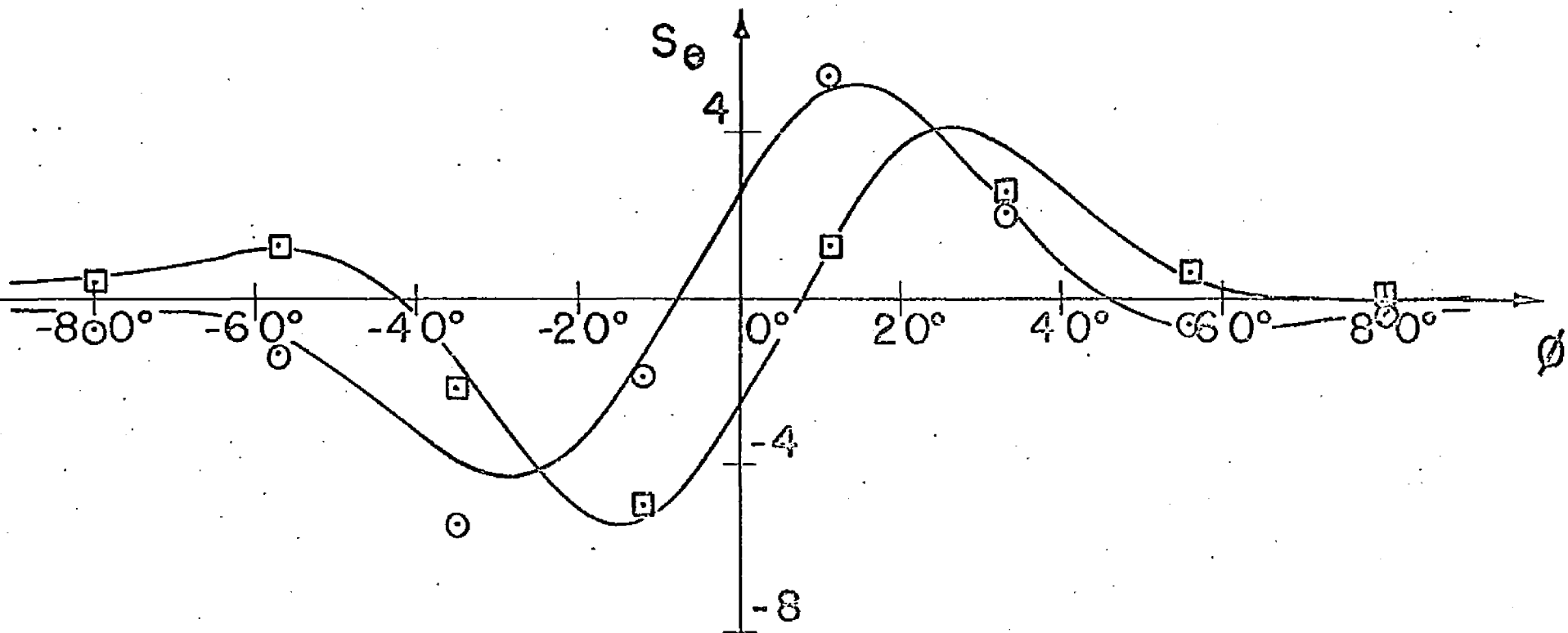
FIGURE 2A



PRESENT THEORY : _____
 EXP. RES. by GROSS & FORD : ○ outer surface
 .. ($\lambda = 0.339, \mu = 36.9$) : □ inner surface

MERIDIONAL STRESS INTENSIFICATION FACTOR

FIGURE 3

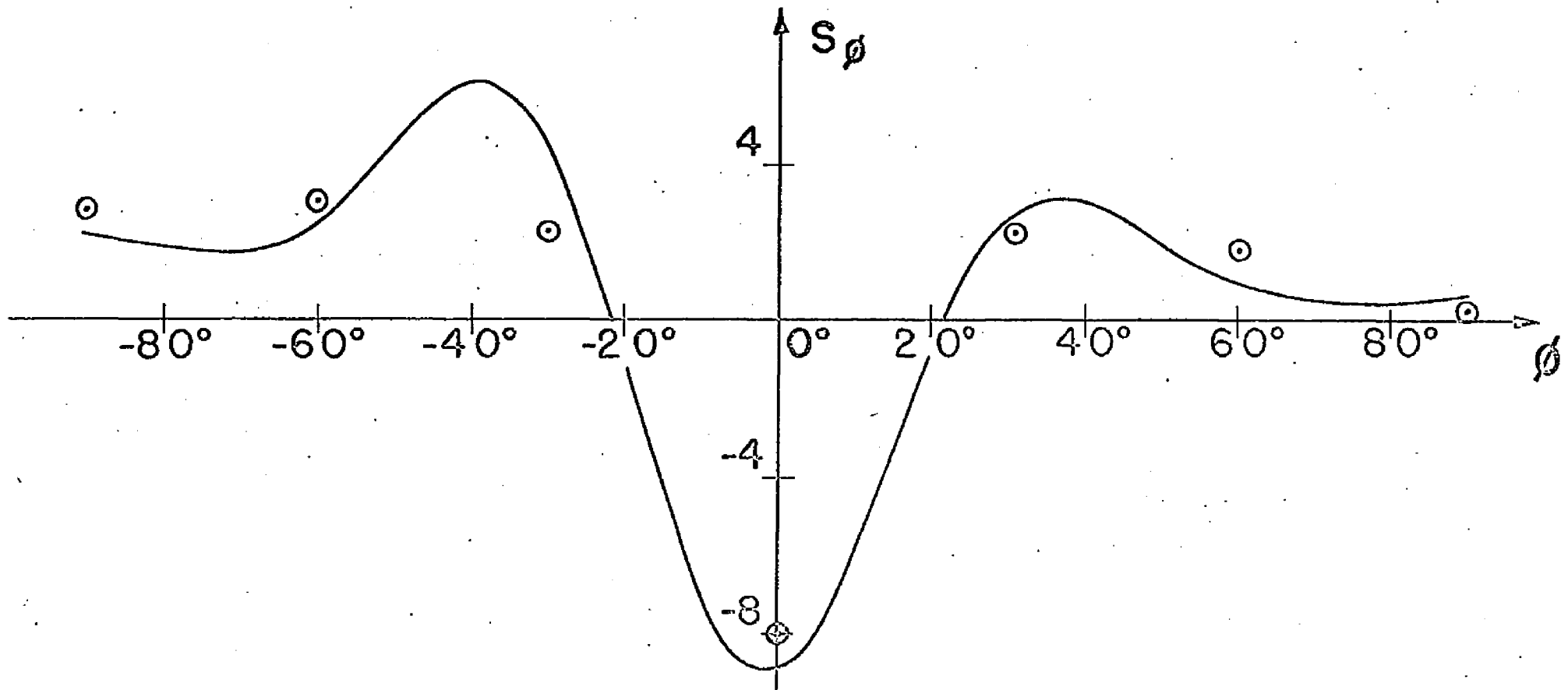


PRESENT THEORY : _____

EXP. RES. by GROSS & FORD : \circ outer surface
 ($\lambda=0.339, \mu=36.9$) : \square inner surface

LONGITUDINAL STRESS INTENSIFICATION FACTOR

FIGURE 4

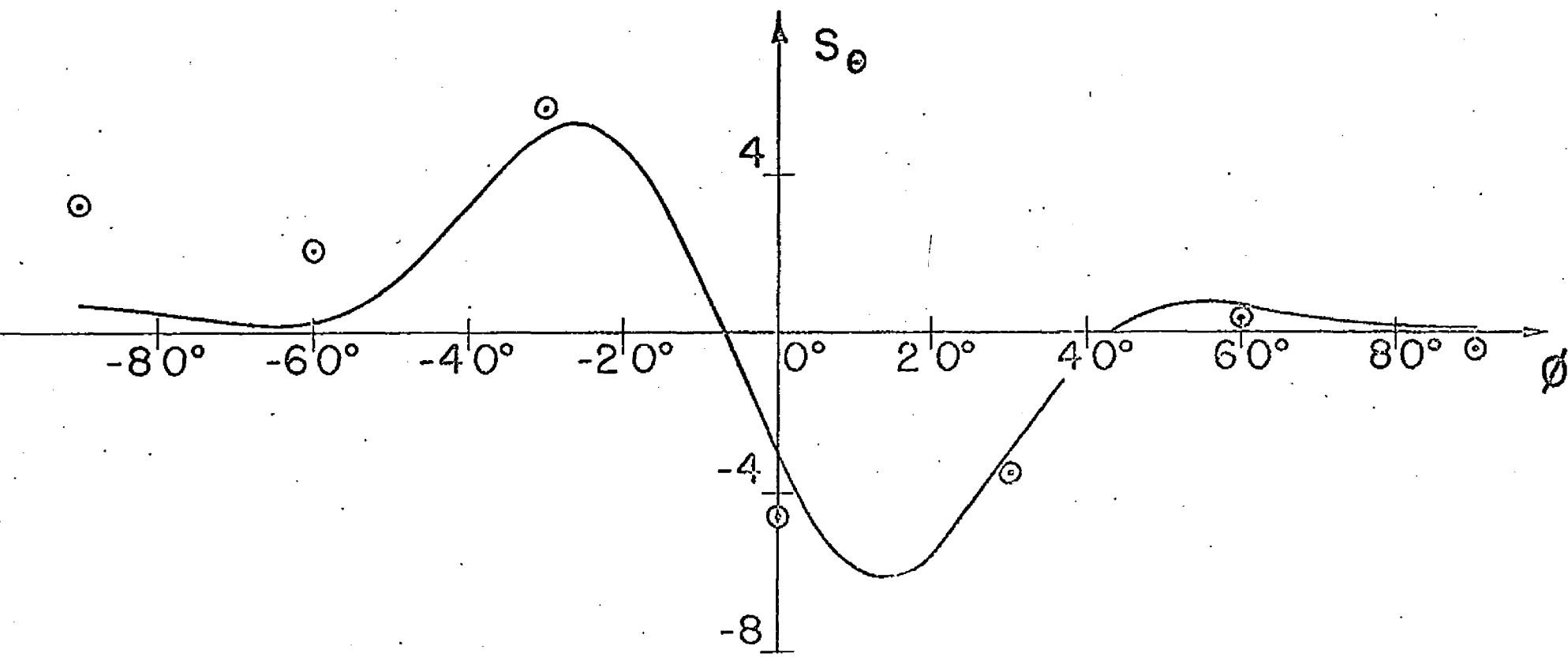


PRESENT THEORY : —————

EXP. RES. by VISSAT & DEL BUONO : \odot outer surface
 ($\lambda = 0.512, \mu = 46.2$)

MERIDIONAL STRESS INTENSIFICATION FACTOR

FIGURE 5

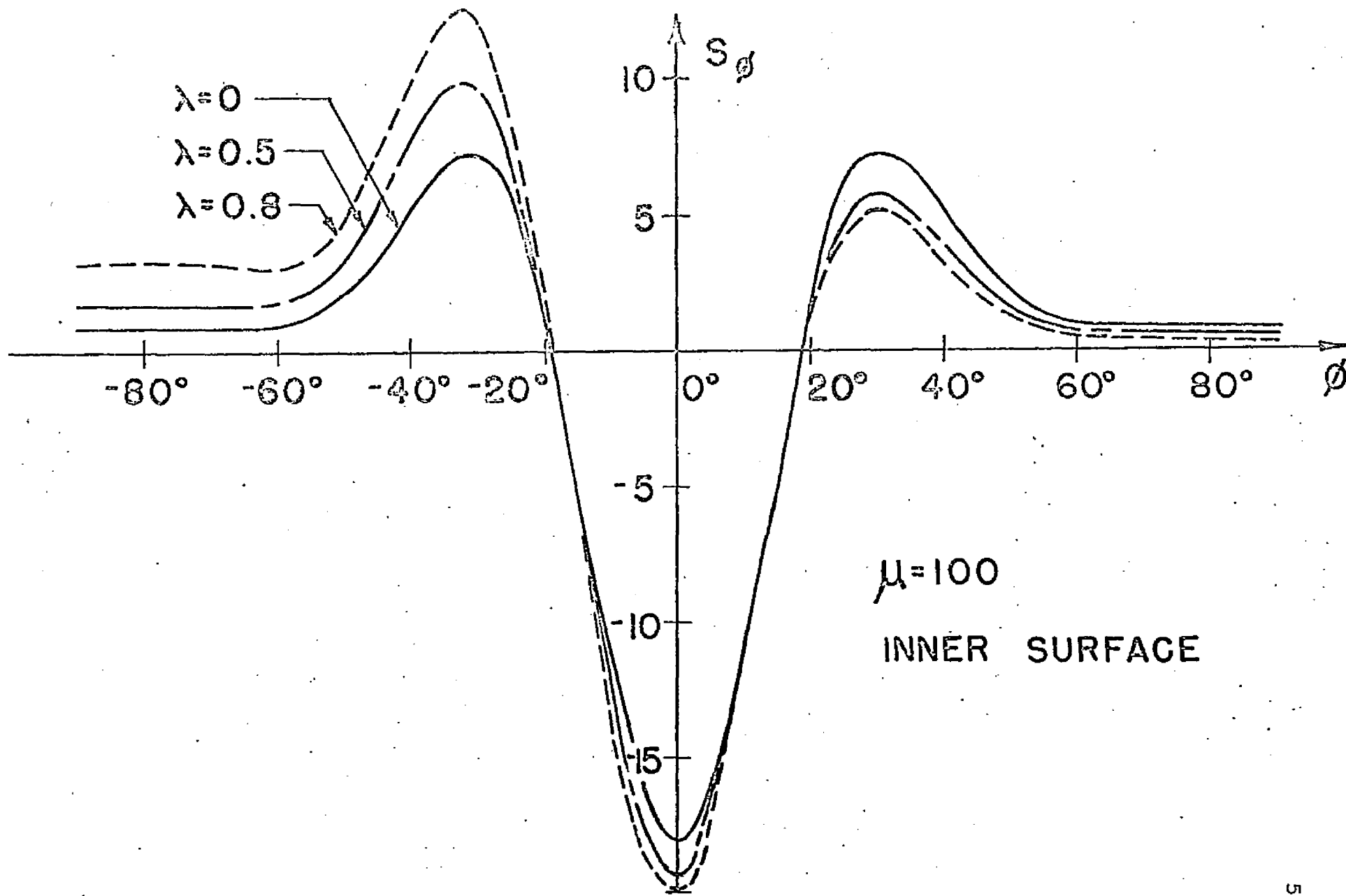


PRESENT THEORY : —————

EXP. RES. by VISSAT & DEL BUONO: o outer surface
 ($\lambda = 0.512$, $\mu = 46.2$)

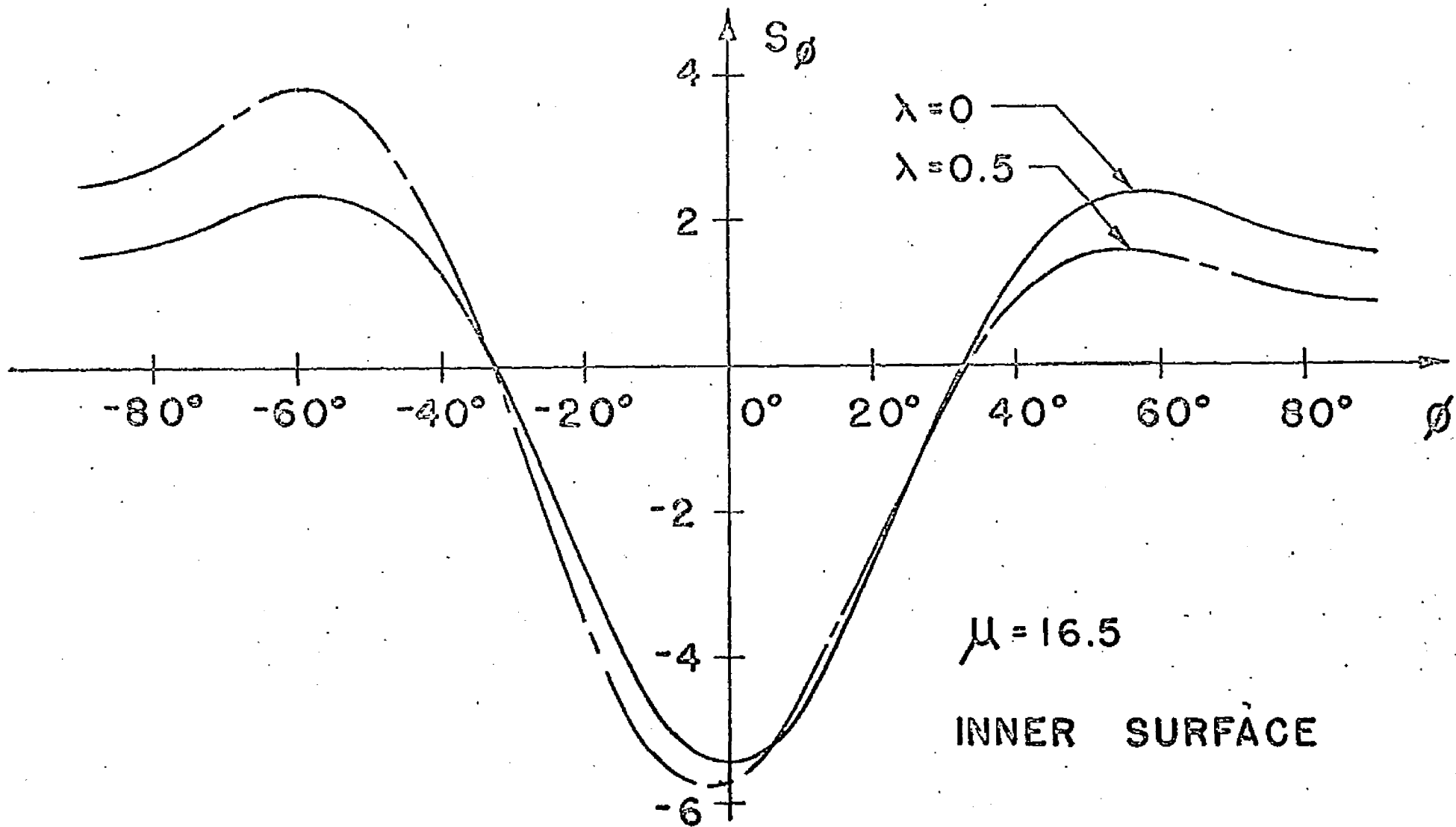
LONGITUDINAL STRESS INTENSIFICATION FACTOR

FIGURE 6



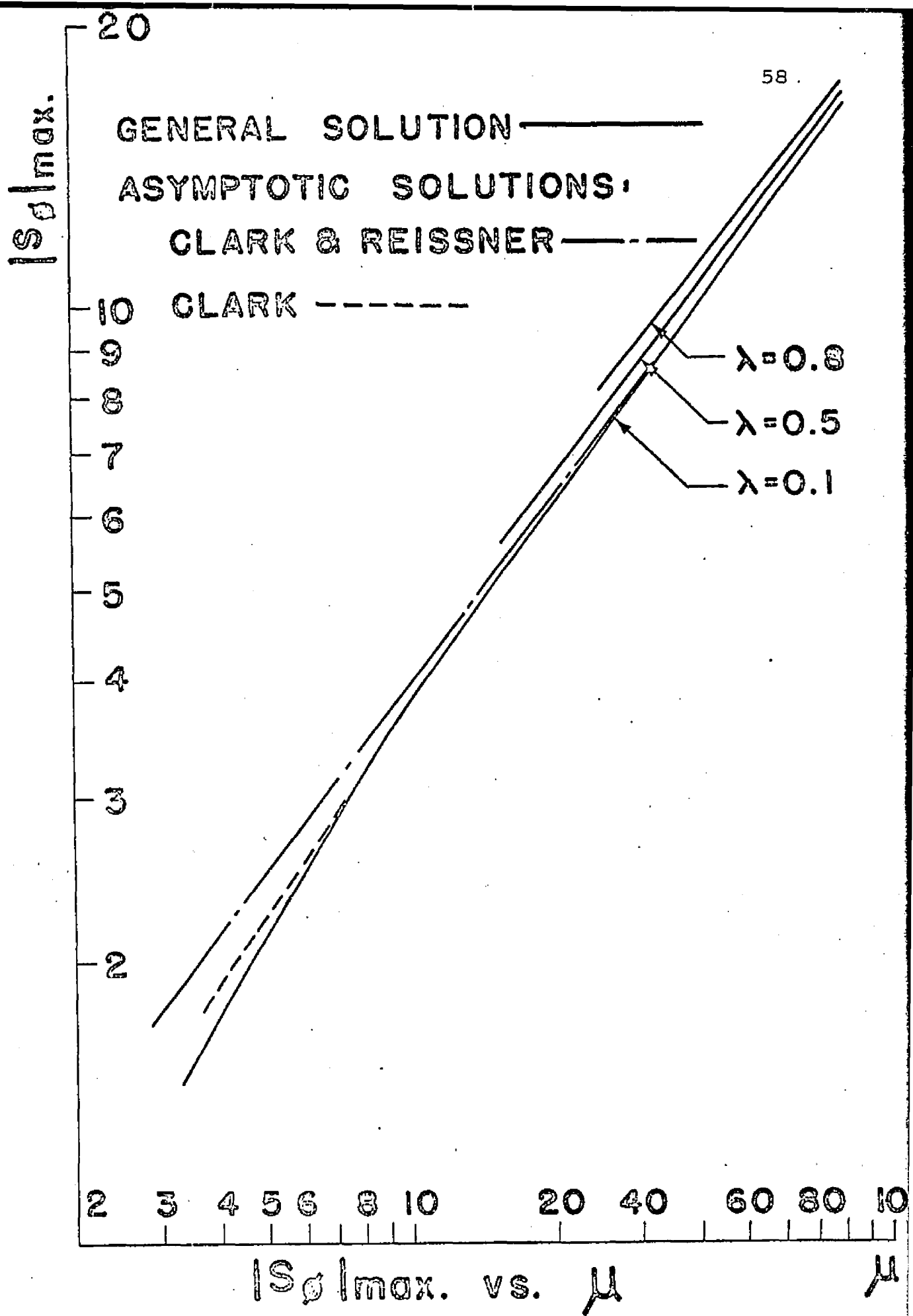
MERIDIONAL STRESS INTENSIFICATION FACTOR

FIGURE 7



MERIDIONAL STRESS INTENSIFICATION FACTOR

FIGURE 8



$|S_0|_{max}$ vs. μ
 FIGURE 9

MODIFIED ASYMPTOTIC SOLUTION: _____

| EXPERIMENTAL RESULTS | Surface | | | |
|----------------------|-----------|-----|-----------|-----|
| | Outer | | Inner | |
| | λ | | λ | |
| | 1/3 | 1/2 | 1/3 | 1/2 |
| GROSS & FORD | □ | | × | |
| PARDUE & VIGNESS | + | | | + |
| VISSAT & DEL BUONO | △ | ○ | | |

20
10
9
8
7
6
5
4
3
2
1

s/ρ_{max}

Inner Surface $\left\{ \begin{array}{l} \lambda = 0.8 \\ \lambda = 0.5 \end{array} \right.$

$\left. \begin{array}{l} \lambda = 0.8 \\ \lambda = 0.5 \end{array} \right\}$ Outer Surface

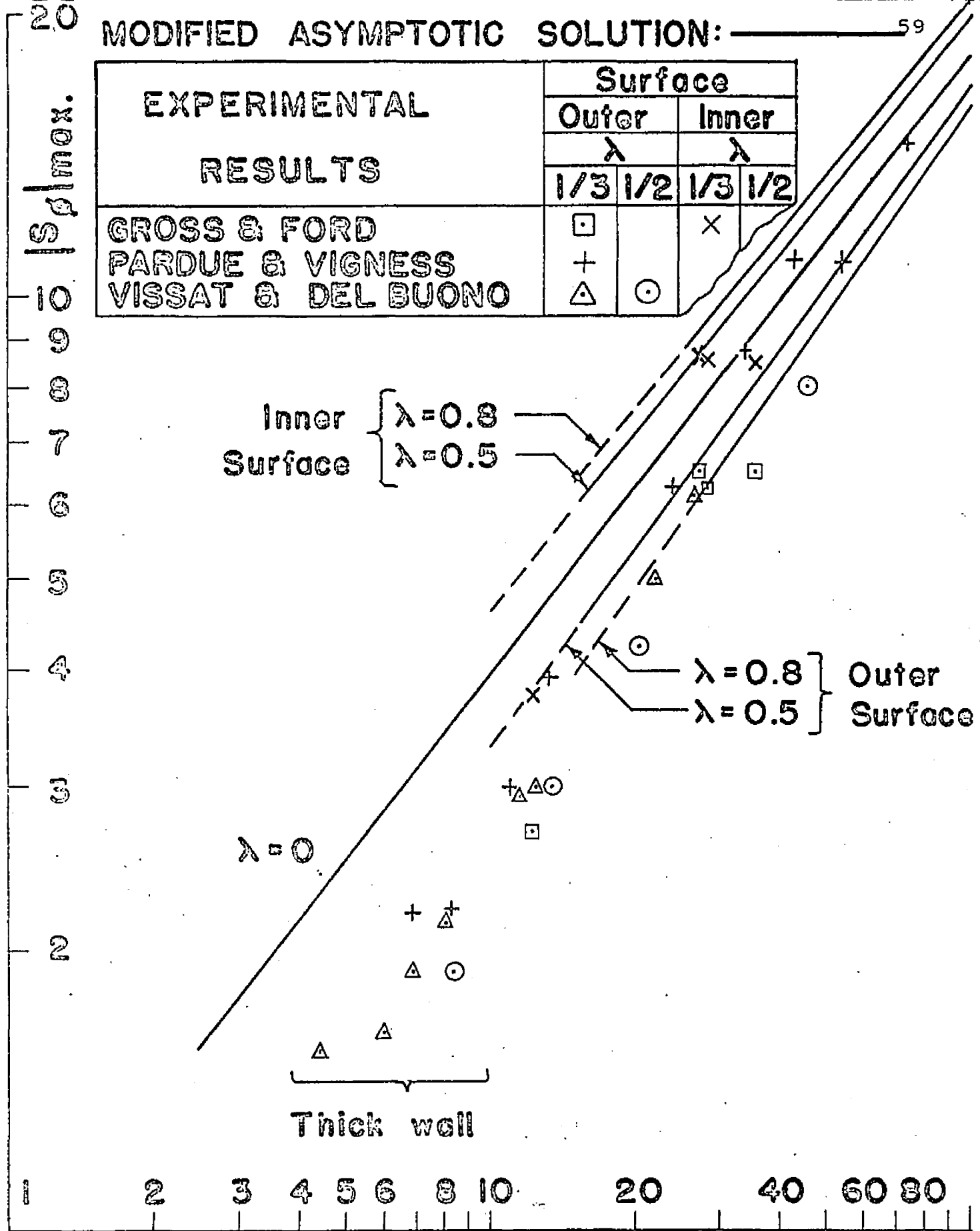
$\lambda = 0$

Thick wall

1 2 3 4 5 6 8 10 20 40 60 80

MODIFIED ASYMPTOTIC SOLUTION μ

FIGURE 10



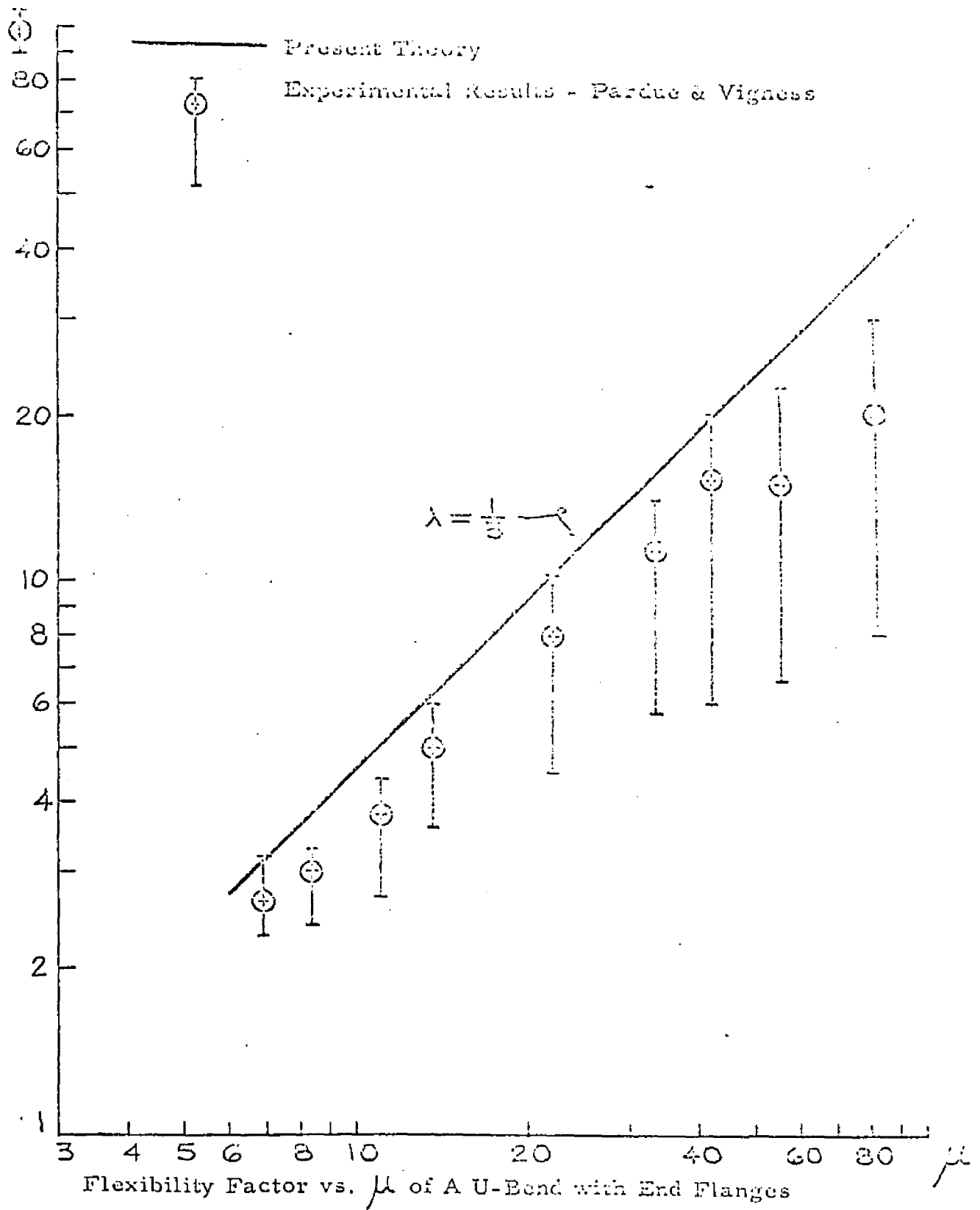


Figure 11

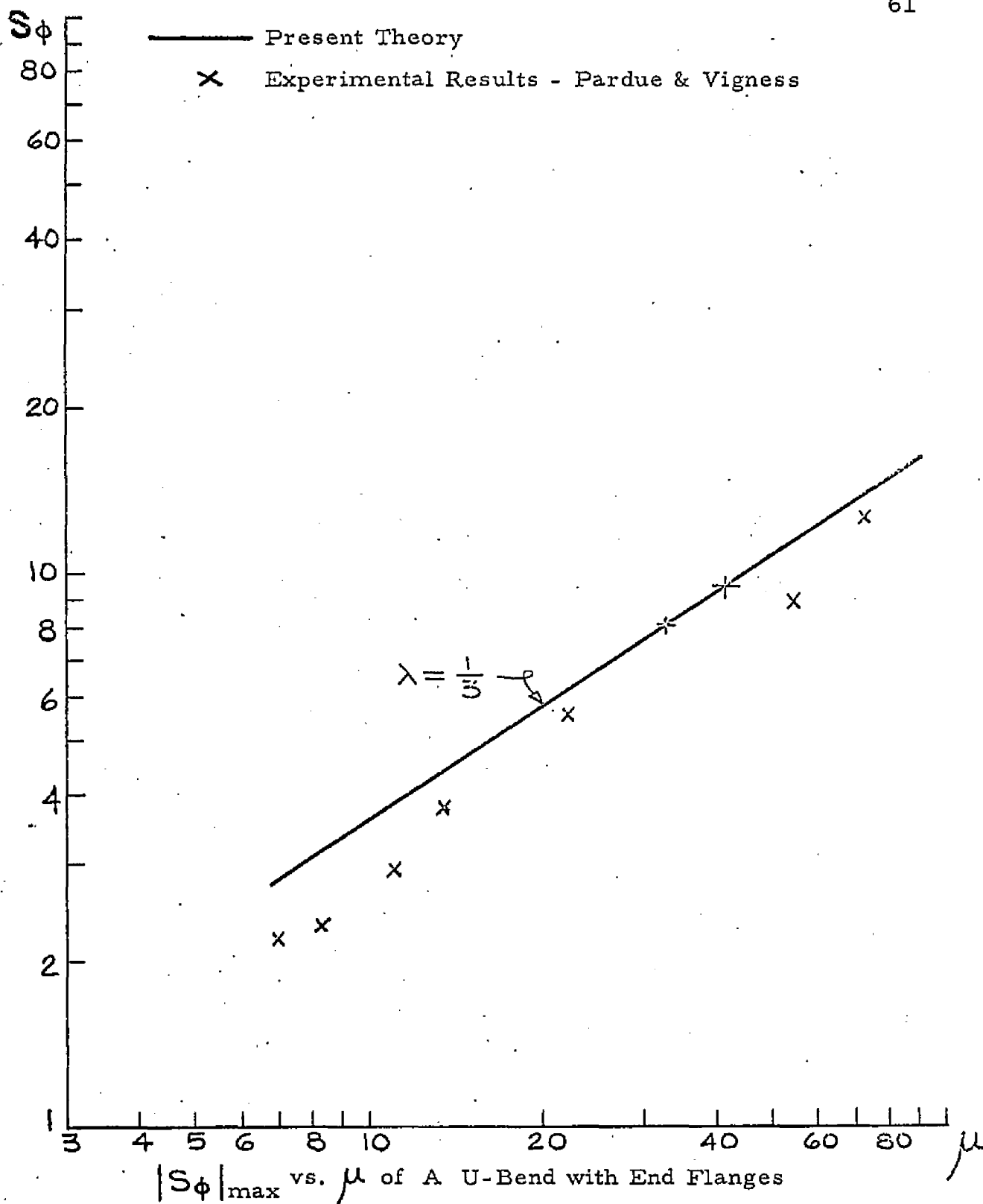


Figure 12

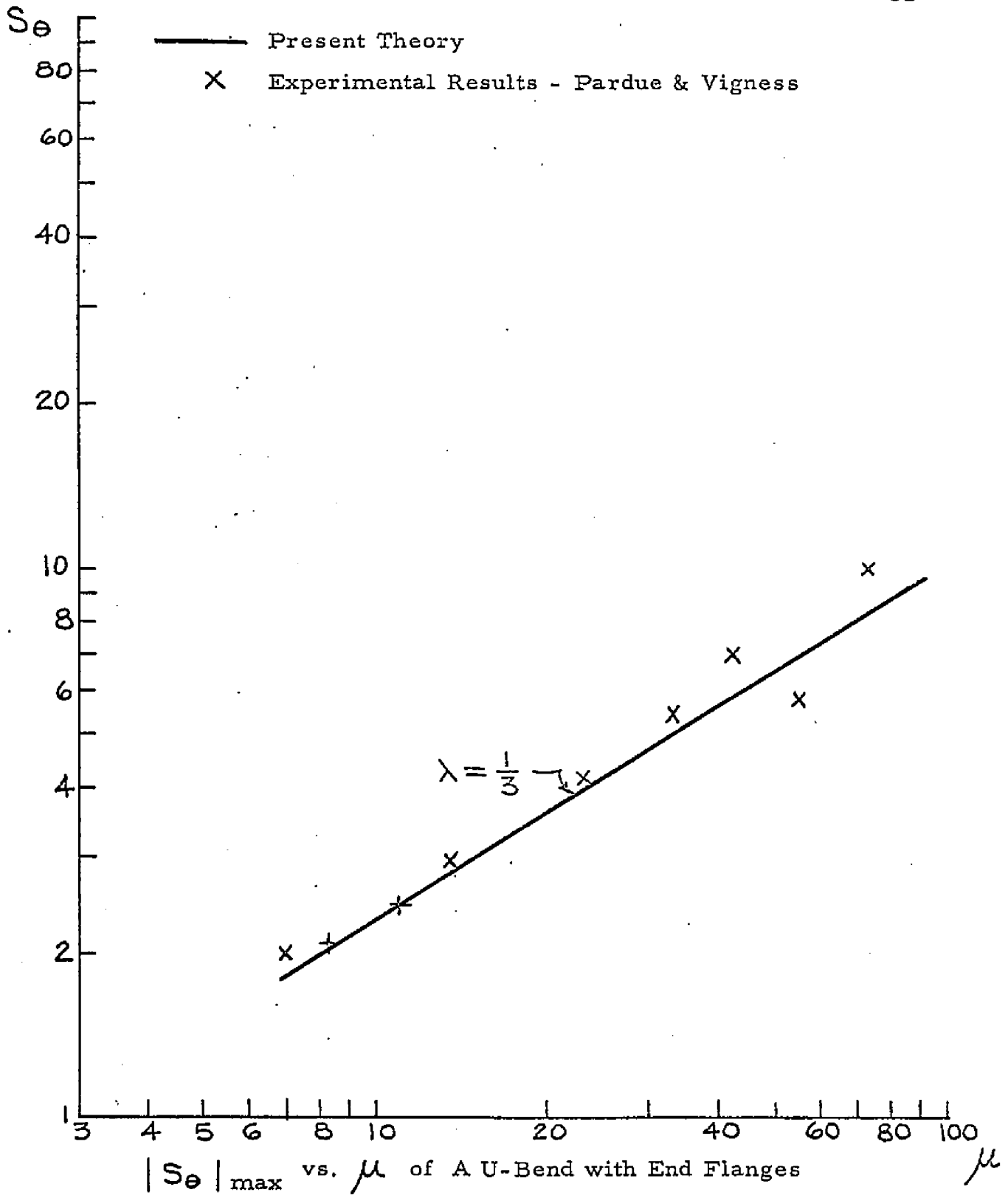


Figure 13

BIBLIOGRAPHY

1. Tueda, M.

Mathematical Theories of Bourdon Pressure Tubes and Bending of Curved Pipes.

Mem. Coll. Eng., Kyoto Imp. Univ., Vol. 8, 102-115 (1934); Vol. 9, 132-152 (1936)
2. Symonds, P. S. and Pardue, T. E.

Characteristics of Short Radius Tube Bends

Second Partial Report, Naval Res. Lab. Report O-2761, 1946
3. Turner, C. E. and Ford, H.

Examination of the Theories for Calculating the Stresses in Pipe Bends Subjected to In-Plane Bending

Proc. Instn. Mech. Engrs., Vol. 171, 513-525, 1957
4. Jones, N.

In-Plane Bending of a Short-Radius Curved Pipe Bend

J. Eng. for Ind., 271-277, 1967
5. Gross, N. and Ford, H.

The Flexibility of Short - Radius Pipe Bends

Proc. Instn. Mech. Engrs., Vol. 1, Ser. B, 480-491
6. Pardue, T. E. and Vigness, I.

Characteristics of Pipe Bends Under Applied Moments

Summary Report, Naval Res. Lab. Report 4253, 1953

7. Vissat, P.L. and Del Buono, A. J.

In-Plane Bending Properties of Welding Elbows
Trans. A.S.M.E., Vol. 77, 161-175, 1955
8. Clark, R. A. and Reissner, E.

Bending of Curved Tubes

Advances in Applied Mechanics, Academy Press, New York
Vol. ii, 93-122, 1951
9. Clark, R. A.

Asymptotic Solutions of Toroidal Shell Problems

Quart. App. Math., Vol. XVI, No. 1, 1958
10. Watson, G. N.

A Treatise on the Theory of Bessel Functions

McMillan, New York 1944
11. Novozhilov, V. V.

Thin Shell Theory

P. Noordhoff Ltd. - Groningen - The Netherlands - 1964
12. Sokolnikoff, I. S.

Mathematical Theory of Elasticity

McGraw-Hill, New York - 1956

VITA

Henry J. Thailer, born in New York City on January 25, 1935, is married and has two children.

He attended Eastern District High School in Brooklyn and graduated in June of 1952. He entered The City College in September, 1952. During this period, he was active in A.S.C.E. student chapter as Corresponding Secretary, elected to Chi Epsilon Fraternity and served in the United States Naval Air Reserve. In June of 1956, he received the Bachelor of Civil Engineering degree Cum Laude.

After graduation, Mr. Thailer worked for the Port of New York Authority, accepted a commission in reserve corps of the U.S. Public Health Service, subsequently was employed by York and Sawyer, and The Public Health Research Institute of The City of New York, Inc. He attended The City College on a part-time basis from September of 1961 until he received the Master of Engineering degree in June of 1964.

In September of 1964, Mr. Thailer accepted the position as full-time Lecturer in the Department of Civil Engineering at The City College and began part-time study toward a Ph.D. degree. Commencing September of 1965, until the Spring semester of 1969, he continued as a part-time Lecturer.

Commencing in the Summer of 1965 and ending in the Summer of 1966, he undertook research on the stress distribution in an elastic body in the vicinity of a crack, under the direction of Professor Leon Y. Bahar, sponsored by the National Science Foundation. He co-authored a technical report entitled "Stress Distribution in Bonded Dissimilar Materials Containing an External Circumferential Crack on Its Interface".

He was the recipient of a Graduate Scholarship award presented by The Engineering Alumni of The City College and obtained his Professional Engineer's license in New York State in 1966.